# MicroObservatory

Honors Project Thesis

Submitted to Faculty of Physics, School of Arts and Sciences

Azim Premji University

In partial fulfillment

of the requirements for the Degree of

Bachelor of Science with Honors in Physics

By Tanishq Sharma

Supervised by Prof. Proteep C.V. Mallik

June, 2020

## Preface

Some time during my second semester, I decided to explore possible honors' project topics by speaking to the members of the physics faculty to allow for thorough consideration before I decided to pick one. In one of the tutorial hours for Mechanics course, while chatting with my professor, I inquired about possible topics for honors and he suggested a project something within the lines of building a telescope or some system to control it. I found this interesting and thought about a project idea within this domain. There were a handful of choices, but one that was a serious possibility of becoming my honors project was building an automatic tracking and mounting system for a telescope. The system could be used to orient a telescope to point at objects or track objects without any manual intervention. I, however, realized that the project was more engineering intensive than physics intensive and decided to do what my current project actually entails. Another option that was seriously considered was manually observing the positions of planets up to Saturn and deriving their equations of motion. This project was not pursued due to limited time of observation that would result in insufficient data relative to the requirements of the task proposed.

This bring us to project I did. In general, for an observatory, a telescope has to be constructed and tested for its quality of observation, some sort of system has to be built and deployed for the type of study or survey that the telescope is intended for, and finally that survey is performed. The reason I decided to name my project MicroObservatory, has to do with that, the project was to entail all of the above

mentioned, just at a smaller scale and at a level of complexity that could be worked with, in an undergraduate laboratory.

During my time working on this project, I had to learn lots of new theoretical concepts, which were important to implement key aspects of the project. I will therefore take the approach in writing my thesis whereby all the theoretical concepts are laid out concisely, before I explain how all these concepts were applied and finally results and data obtained during the project will be presented.

Before I begin with the scientific content, I would like to express my gratitude to my supervisor Prof. Proteep for all his guidance and advice throughout the project, while simultaneously allowing me to work at a highly independent level in terms of how to direct and navigate the project forward. His knowledge and understanding for modifications of certain goals in the project were vital. I would also like to thank our Physics TA Mrs. Manoja for helping me with procurement of key equipment and also for her advise during certain experimental aspects of the project, and Prof. Rajaram for his guidance prior to the start of the project.

Tanishq Sharma

## Table of Contents

## Abstract

The project detailed in this thesis has been a culmination of working with aspects from the field of astronomy, optics and computer science. The project's goals included building and testing a Newtonian Reflector telescope, and building a system that would be added to the telescope for mapping celestial bodies.

The process of building the telescope includes optical modelling of the primary mirror that was to be fitted into the telescope, followed by grinding and polishing of the glass blank that would later have to be aluminized to make it into a mirror. This mirror could later be fitted into a telescope that was built based on the optical model designed. The mirror that was worked with was prepared to be an 8 inch f 8.8 parabolic mirror. There were some difficulties experienced in the final stages of the polishing which meant the mirror could not be aluminized and fitted into a telescope (explained in detail in Chapter 4).

The process of testing the telescope includes testing the optical quality of mirror being made. This can be done in multiple ways. Some methods are more fundamental and are used during the process of grinding and polishing while others are thorough tests done during the end or near the end of polishing. These thorough tests include qualitative tests like the star test and quantitative tests like the Foucault knife edge test. All the testing that was done was done by apparatus that was readied in the lab itself. There are multiple facets to the results that were obtained using these tests that are available in thorough details in Chapter 7. However, the key results out of the testing include the characterization of the shape of the surface profile of the

mirror. The surface of the mirror was found to have a conic constant of -1.448 with a Strehl Ratio of 0.95.

The process of mapping celestial body includes using an inertial measurement unit board composed of multiple sensors, and interfacing it with a microcomputer followed by writing a program that could use values obtained from the microcomputer, and using local data such as time, location, etc. to obtain the celestial coordinates of an object being viewed with the telescope. This system was successfully built, thoroughly tested and implemented on an existing telescope in the university. The sources of error resulted from inaccuracies while centering an object within the field of view of the telescope and random noise within the data. The first source of error contributed to far less compared to the latter. For a single data point, the error could be as high as a couple of degrees. However, the inherent randomness of noise means a large number of data points could be averaged out to get fairly accurate results, which is exactly what was done while mapping the celestial bodies. The results can be seen in Chapter 8 on Star Catalogue and Sky Map.

This concise introduction to the project should suffice for the time being, until the reader reads through chapters 1, 2 and 3 which will go over the theoretical concepts in greater details, followed by chapter 4, 5 and 6 where information pertaining to physical aspects of the project will be covered in greater details.

## Chapter 1: Astronomy Basics

The universe has 3 spatial dimensions in which masses interact with one another due to multiple types of phenomena at work depending on length and time scales. In astronomical observations, observed acceleration of a body can be due to two factors, geometry of spacetime (gravitational force) or expansion of space. Both these phenomena are observable, but require very sensitive equipment making measurements over a long time of period (unless one is dealing with very close objects like nearby planets or satellites). The ambiguity due to the use of relative terminology is deliberate, as these complex aspects are beyond the aspect of this project.

From the above paragraph, it becomes a little obvious that within the scope of this project, celestial bodies will be viewed as 'stationary' objects. Before going any further, one more simplification needs to be made, which may initially seem extreme, but has worked for ancient astronomers for centuries. By looking at stars, or other celestial bodies, there is no simple way to know how far they are from us, the observers on Earth. There are techniques such as by measuring the redshift or blueshift of the spectra of a star, etc. but they are recent areas of research requiring fairly modern technology. For ancient astronomers, it was reasonable to think of all stars being very far away from us (that we assume that distance to be infinity). Since all celestial bodies are infinitely far away from us, we could assume a sphere of infinite radius has celestial bodies embedded in it, and we are located right at the center of sphere. This geocentric sphere is called the Celestial Sphere.

Before getting into further details, one should note the following: almost all objects on celestial sphere appear to be exactly where they are over not just months or years, but decades. One could spend an entire lifetime observing the celestial sphere and not see any difference in relative positions between most objects, unless using recent technology of course. The major exceptions to this rule include moon, which is very different to any other celestial object based on its apparent size and apparent brightness, planets and other satellites. Planets appear similar to stars, but they move around on the celestial sphere and it is therefor that ancient astronomers called them planets, based on planētēs, i.e. wanderer in Greek. They wandered around when everything else was stationary.

This idea of observing the sky and seeing almost every object maintain its position relative to every other object has good implications, as one could create a map of celestial objects by making observations and then using it to be able to locate celestial bodies. One could also use it to answer other interesting questions, such as telling the local time or local coordinates depending on the other piece of information one has. Putting these implications aside for a while, it is time to look at how one would map the sky first.

A good way to start mapping the sky would be to take clues from how Earth is mapped. A map of Earth is generally constructed in two dimensions (disregarding topographical features of the land) and same would be true of the Sky as distance to objects is disregarded by assuming all celestial objects to be at an infinite distance. Hence it is necessary to have two coordinates to be able to uniquely identify point on a map. Before going onto defining this coordinate system, one should take a look at

the spherical polar coordinates system. Whereas in a three dimensional cartesian system, one would use the x, y and z axis to locate a point, in spherical polar, one uses r, θ and ϕ. For a sphere, r, the distance from origin is fixed. To uniquely identify any point on the sphere, only θ and ϕ are needed. However, an important thing to note is that the polar angle, θ goes from 0 rad to π rad whereas the azimuthal angle ϕ goes from 0 rad to 2π rad. Furthermore, there are two terms to understand, great circles and meridians. When a plane intersects with a hollow sphere such that it passes through the center of the sphere, the points of intersection form the great circle. If one takes exactly half of this circle, one gets a meridian. It should come as no surprise that to define coordinates on a two dimensional spherical map, the reference to any point should be from a well defined great circle and a well defined meridian .

This is exactly what happens on an Earth's map, the reference to any point is given based on latitude, which is a measure of angle from Equator (a great circle) and longitude, which is a measure of angle from the Greenwich Meridian (a meridian). The reason we explicitly mentioned reference lines for an Earth's map is that we take 3 important aspects from it and map it to the celestial sphere. Firstly, if one considers and infinite plane, that upon intersecting the Earth gives the equator, this exact same plane intersecting with the celestial sphere gives the celestial equator. An easy way of conceptualizing this idea is to think of Earth's equator as a circle with radius r, that is the radius of the Earth, and mapping this circle onto the celestial sphere by increasing r from approximately 6378 km to ∞ km. This gives us the first aspect. Secondly, an infinite straight line passing through the North Pole and South Pole would intersect the celestial sphere at two points, the one on the northern side being

the North Celestial Pole, and the one on the southern side being the South Celestial Pole.[1] This gives us the second and third aspect. On Earth we have the Greenwich Meridian going all the way from North Pole to South Pole, and similarly on the celestial sphere, the reference meridian goes all the way from the NCP to SCP. To define a meridian, one needs to understand a few astronomical terms, which are made clear with the use of pictures.

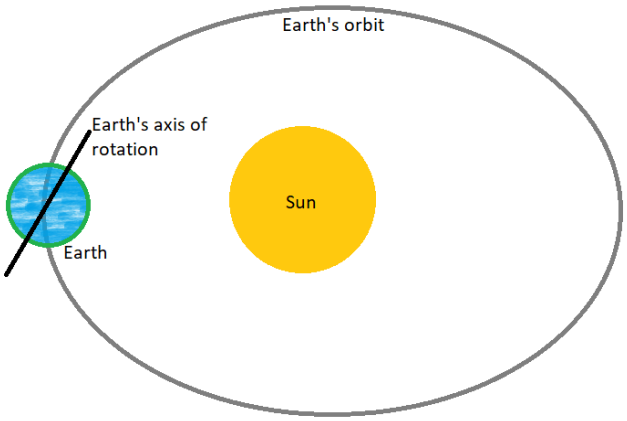


Fig 1.1: Earth's Orbital Plane

As the Earth orbit's around the sun, the orbit itself can be considered to be a closed one (for our purposes) and the orbit defines an orbital plane.

If the orbital plane extends to the infinity, it will intersect with the celestial sphere at what is shown as the ecliptic, in the image of the celestial sphere.

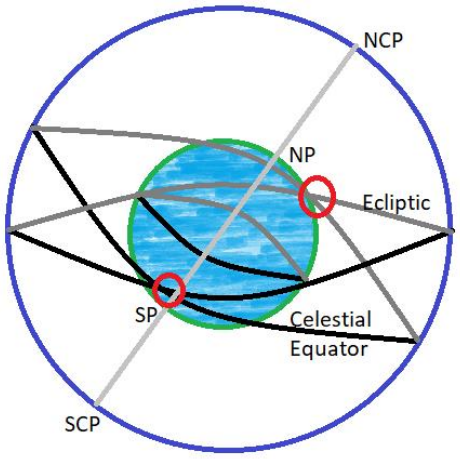


Fig 1.2: Celestial Sphere

[1] The North and South poles specifically refer to the true North and true South poles and not the magnetic North and magnetic South poles due to variability in position of magnetic poles.

Before moving on, it is important to understand the significance of the ecliptic. Ecliptic is the exact path the sun traces over a period of year. To demonstrate why this is the case, a picture might help.

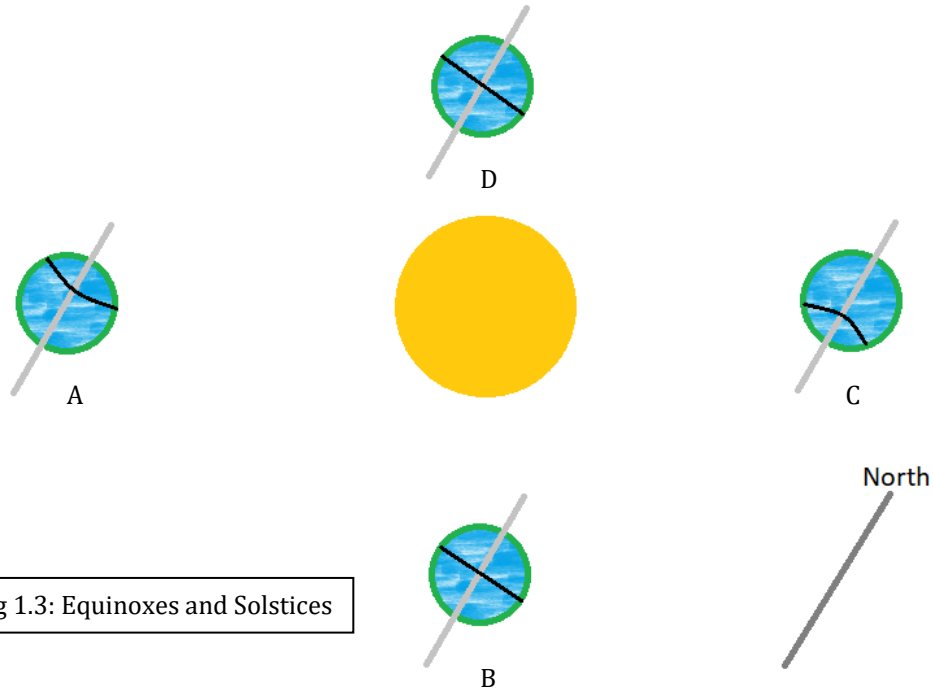


Fig 1.3: Equinoxes and Solstices

In the image, Earth is shown at 4 different points along its orbit. Due to the tilt of its axis, Sun is exactly overhead to specific latitudes at specific times during the year. The range of these latitudes is 23.4° N to 23.4° S. Therefore, over a period of one year, the sun appears to trace the ecliptic on the celestial sphere. During this annual journey along the ecliptic, there are 4 important days: Summer Solstice (as shown in A), when the Sun is at the Northmost position, Winter Solstice (as shown in C), when the Sun is at the Southmost position, Autumnal Equinox (as shown in B), when the Sun is at the Equator and Vernal Equinox (as shown in D), when the Sun is, again, at the Equator. Over a period of a year, Summer Solstice, Autumnal Equinox, Winter Solstice and Vernal Equinox are observed in this specified order. The naming of these days has to

do with geopolitics, hence I will refrain from going into that. The points marked in red in Fig 1.2 are the equinoxes on the celestial sphere.

It is now possible to define the lines used on the celestial sphere for referencing any specific point. The celestial equator is the great circle that will be used. The meridian is defined such that in includes the North Celestial Pole, the Vernal Equinox and the South Celestial Pole. The choice of equinox is rather arbitrary and autumnal equinox would equally work for the meridian but nevertheless, this specific convention should be followed because it is this specific meridian that is followed by all the scientific literature.

Now that the two reference lines have been defined, it is possible to define the coordinate system. Just as Earth maps have latitude and longitude, Celestial maps have Declination and Right Ascension. Declination lines are circles, analogous to latitude circles, on the celestial sphere with the reference line being the celestial Equator. Right Ascension lines are meridians, analogous to longitude lines, on the celestial sphere with the reference line being the NCP-Vernal Equinox-SCP meridian.

The declination at the celestial equator is defined as 0°, it increases in the northward direction with the North Celestial Pole being at a declination of 90°, and it decreases in the southward direction with the South Celestial Pole being at a declination of -90°. However, when a declination is being specified, it is specified in a tricky manner. 1° is defined as 60 arcminutes (denoted as 60') and 1' is defined as 60 arcseconds (denoted as 60"). Thus, a declination of 47.53° will be written as 47° 31' 48". For increasing accuracy, decimal system is used in arcseconds, for instance,

47.539° will be written as 47° 32’ 20.4”. This is purely a matter of convention and due to computational reasons, I have refrained from using arcminutes and arcseconds and instead used degrees with decimal points for the purpose of specifying declination in results.

The right ascension is defined as 0° on the NCP-VE-SCP meridian, and it increases in the eastward direction until it reaches 360° which is the same specified meridian. An interesting observation is that, whereas all points of the celestial sphere are defined by two coordinates, the declination and the right ascension, at the NCP and SCP, this isn’t the case. Due to the way the meridians are defined, all of them pass through NCP and SCP, hence these points are just 90° and -90°, and asking for their right ascension does not make sense. The convention of specifying the right ascension is again, a little tricky. 15° equals to 1 hour, 1 hour equals to 60 minutes and 1 minute equals to 60 seconds. Thus, a right ascension of 197.43° will be written as 13 09 43.2. The increasing accuracy can be taken care of by adding more digits after the decimal point in the seconds. In this project, this system is used as per convention.

It is possible that there might be a little confusion regarding all these defined units and hence it might help to look at the following table.

| Specified Unit | 1’ (arcmin) | 1” (arcsec) | 1 hour | 1 minute | 1 second |
|---|---|---|---|---|---|
| Value in degrees | $1/60$ | 1/3600 | 15 | $1/4$ | $1/240$ |

Table 1.1: Degree conversions

With the celestial coordinate system defined, there are a number of concepts that need to be understood. For any observer, the celestial sphere will appear to move

as the Earth rotates. The point on the celestial sphere that is directly overhead of an observer is called the Zenith. The point that is direct below the observer is called the Nadir. For every observer at every point of time, half the celestial sphere is in sight, ignoring the obstructions on ground. The border of visible parts of celestial sphere is called the Horizon. The way the coordinate system is defined is such that, for any observer fixed to their position on Earth, the declination of their Zenith is constant. For an observer located at 34° N, 120° E, the declination of their zenith will always be 34°, similarly, for an observer located at 79° S, 2° E, the declination of their zenith will always be -79°. The zeniths at North Pole and South Pole are NCP and SCP respectively. However, for every observer, the right ascension of their zenith continuously changes, due to Earth's rotation. The right ascension of the zenith, for any particular observer, is their sidereal time, or local sidereal time.

In general, with the assumptions made in the above definitions and explanations, the RA and Dec[2] for any celestial bodies (except planets, satellites and the Sun) is fixed irrespective of the position of the observer on Earth. Furthermore, for an observer on the NP, only celestial bodies between Dec of 0° and 90° will be observable. Similarly, for an observer on the SP, only ones between Dec of 0° and -90° will be observable. For an observer on the equator, the entire celestial equator is observable. However, whether any particular celestial body, given it falls in the observable range for the observer's position, can be seen or not depends on the position of Sun on the celestial sphere, i.e. the time of the year.

[2] From here onwards, declination will be referred to as Dec and right ascension as RA.

## Chapter 2: Fundamentals of Telescopes

With the notion of the celestial sphere developed, it is time to understand the equipment used to observe the celestial sphere. Astronomical observations can be made using cameras, binoculars, telescopes and obviously, eyes (the only method of astronomical observation for millenniums). In this chapter, the focus will be particularly on telescopes. Telescopes, however, are not just limited to optical observations. Telescopes can be built for optical or radio astronomy if they are to be operated from Earth, and/or include other sections of the electromagnetic spectrum if they are to operate in space. The focus here will be on optical telescopes.

An optical telescope is used for collection of electromagnetic waves that lie in the visible part of the spectrum. The reason one would use an optical telescope over one's eyes to make observations has to do with the aperture and the amount of light. The pupil in human eyes have an aperture of a few millimeters. The aperture of an optical telescope would generally start from the range of few tens of millimeters up to a few meters. Given that area increases as square of the radius of the aperture, a 2 inch or ~ 50 mm telescope will collect roughly 100 times more light than a human eye with its pupil dilated to 5 mm diameter. It is this extra light that one is after while using a telescope. Contrary to popular belief, the purpose of a telescope is not higher magnification but rather higher light gathering capability. More light means more information thus it allows for higher magnification as a result. More light doesn't just allow for higher magnification but also allows for viewing of faint objects.

This brings us to the mechanism of a telescope.[3] Telescopes need to have some sort of converging mechanism such that all the light entering through its aperture converges to a single point of focus. It is here that lenses and mirrors come into use. A telescope is made with at least one, and generally multiple optical equipment, i.e. lens/mirror. A requirement for telescopes is that the optical surfaces have to be smooth to the order of hundreds of nanometers at least or even tens of nanometers. To be able to make equipment with such smoothness, mirrors are easier to deal with as compared to lenses provided a mirror has only one surface whereas a lens has two. This is precisely the reason that for larger telescopes, the primary piece of optics is a mirror despite lens being the one that would generally provide for better quality images. A mirror is easier to manufacture and can also be made to be lighter as compared to a lens for a same aperture size telescope.

A telescope with a primary lens is called as a refracting telescope whereas a telescope with a primary mirror is called a reflecting telescope. A mirror which combines both is called a catadioptric telescope. The focus in this chapter will be on reflecting telescopes. The category of reflecting telescopes is quite large, with there being many types of such telescopes. One of the most common among them is the Newtonian Reflecting Telescope. This is the telescope that was designed as part of this project and hence it is this telescope, for which theoretical aspects will be laid out in this chapter.

[3] From here onwards, a telescope refers to an optical telescope, unless specified otherwise.

A Newtonian Reflecting Telescope has 3 main optical parts, a primary mirror, a secondary mirror and an eyepiece. The primary mirror is a concave mirror positioned perpendicular to the optical axis. An optical axis is the axis along which light waves propagate. This causes the light to converge, however the focal point would then be just above the mirror. Since it would not be ideal to look at this focal point, as the obstruction of one's head would block most of the light, a flat secondary mirror which is much smaller than the primary mirror is placed at a 45° angle to the optical axis prior to the focal point. This allows the converging beam to travel in a direction perpendicular to the optical axis of the telescope and the beam continues to converge, until it hits the eyepiece which has two lenses. One lens is used to diverge the beam based on its focal length (thus causing the magnification) and the other lens collimates the light to form the image that is actually projected to the observer's eye. The following is a simple schematic of how a Newtonian Reflecting Telescope works.

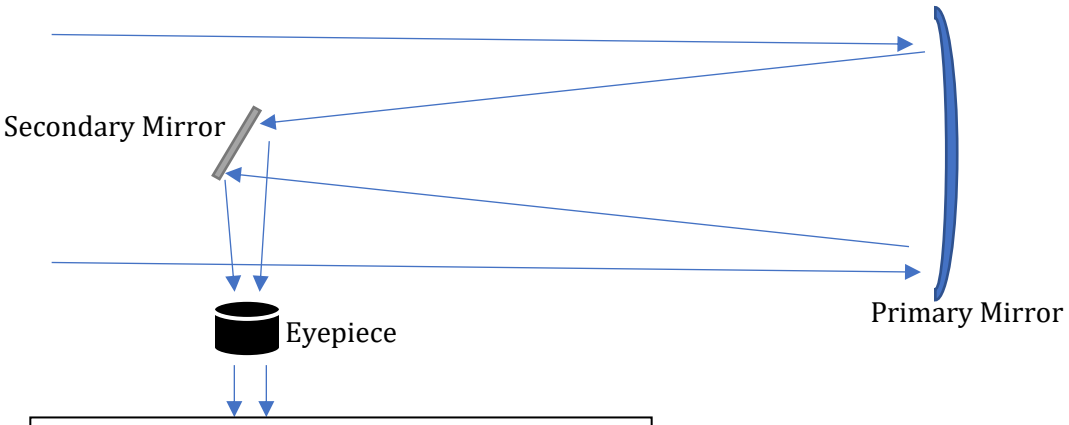


Fig 2.1: Newtonian Reflecting Telescope Schematic

It is important to understand certain properties of the optical surfaces to effectively model the telescope one intends to finally build. However, before these properties are introduced, it is important to understand the surface profile of the

primary mirror. The primary mirror has a circular footprint and a concave reflective surface. The question then arises as to which kind of a concave surface is needed for the mirror. This is derived mathematically. Consider the diagram below:

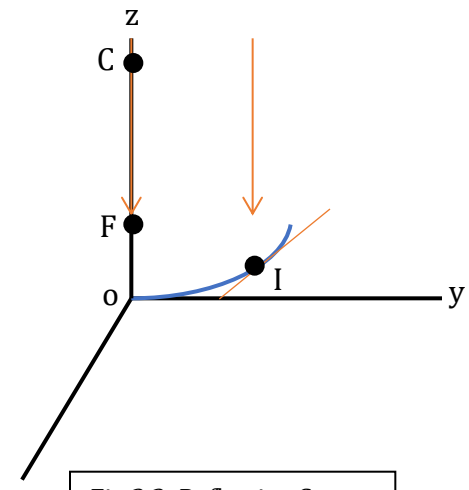


Fig 2.2: Reflective Curve

The blue curve shown above lies on the z-y plane. Almost all mirrors/lenses have symmetry about their optical axis (z-axis) hence by rotating this blue curve about the z-axis, a concave mirror can be generated. Given the symmetry, the following arguments that are made for this curve will hold for the concave mirror. The point I is an arbitrary point on the curve being hit by an incident beam of light that is parallel to the optical axis. This point has coordinates (0, y, z). There is another beam of light striking the blue curve that is passing through the optical axis. The reflected ray of point I, and the reflected ray of origin, meet at F (0, 0, f). The incident ray at I, and the line FI have an angle of 2θ between them. The point C (0, 0, c) is such that ∠FIC is θ. The orange line passing through I and y-axis is the line tangent to point I on the curve. The angle the tangent makes with y-axis happens to be θ given how the figure is defined. This means the derivative at I, $dz/dy = \tan(\theta)$. Since both the

incident rays are parallel, ∠FCI is θ. If we define a point Z (0, 0, z) such that ∠OZI is π rad, then ∠ZFI is 2θ. Based on all of the above:

$|OF| = f = z + \frac{y}{\tan(2\theta)} = z + \frac{y(1-tan^2(\theta))}{2\tan(\theta)}$ where f is called the focal length.

This formula for f that has been derived will now be applied to two surfaces, a spherical one and a paraboloid. The results will explain the choice of these two surfaces. Firstly, for the spherical mirror, note that CI is perpendicular to tangent at I, and C is the center of the sphere. Take CI to be r. Also note that FI = FC which can be taken as a. Using law of cosines, $r^2 = 4a^2\cos^2\theta$ and hence $a = r/2\cos(\theta)$. Since,

$$f + a = r, f = r\left(1 - \frac{1}{2\cos(\theta)}\right)$$

This is the equation for the focal length of a spherical mirror. For a paraboloid mirror, consider the curve to be a parabola, having the equation $z = Ay^2$. Then $dz/dy = 2Ay$. By substituting this into the general equation for f derived above,

$$f = Ay^2 + \frac{y(1-4A^2y^2)}{4Ay} = \frac{1}{4A}$$

This is the equation for the focal length of a paraboloid mirror.

It is now possible to understand the properties of mirrors. Firstly, consider f for a spherical mirror. The equation contains θ, which implies f changes based on θ and hence a spherical mirror does not have a single focal point. However, if small angle approximation is made, then $2f \approx r$, i.e. the focal length is half of the radius of curvature for a spherical mirror. Secondly, a parabola does not have a center of curvature, however, its focal length is a constant as shown above. In general, a

spherical mirror does not have a unique focal length and a paraboloid mirror has no center of curvature, however, for the purposes of a primary mirror, we define a focal length and a radius of curvature for both types of mirrors as follows: for spherical mirror, focal length is half of its radius of curvature and for a paraboloid mirror, radius of curvature is double that of its focal length.

A unique focal point ensures that the reflected image is sharp and clear. This makes a paraboloid mirror (surface with a conic constant -1), the ideal mirror for a telescope. However, spherical mirror (surface with a conic constant 0) is simpler to make whereas making a paraboloid mirror requires complicated figuring of a spherical mirror. It is thus decided based on the specifications of the telescope whether to use the spherical mirror directly (if the focal length is sufficiently long and the small angle approximation is a good approximation to make) or to parabolize it first (if the focal length is quite short and small angle approximation is not ideal). It is important to note that in general, the maximum difference (in terms of maximum gap between two surfaces if they share the same origin as the center of the optical surface, and the same alignment) between a spherical mirror and a paraboloid mirror is in the order of a few hundred nanometers.

Consider the beam reflected off the primary mirror. This beam is a circle at all points until it reaches the focal point, where it is a single point. The secondary mirror is tilted at 45° from the optical axis. From the perspective of the primary mirror, the secondary mirror appears to be a mirror with a circular footprint having a diameter d. However, given its positioning and the shape of the reflected planar beam, d

corresponds to the minor axis of the secondary mirror and its major axis turns out to be d*$\sqrt{2}$. The secondary mirror has an elliptical footprint. The beam reflected off the secondary mirror strikes enters the eyepiece, and exits the eyepiece for the observer to see. The eyepiece has a certain focal length. The focal length of the primary mirror divided by the focal length of the eyepiece gives the magnification of the setup. This wraps up the theoretical concepts of optics of a telescope, that will be extensively used in Chapter 4.

Another important aspect of a telescope is its mount. The two commonly used types of mounts are the Equatorial mount and the Altitude Azimuthal mount. These mounts have subcategories based on different designs. What separates these two types is the way they approach the method of positioning a telescope to a celestial body. In general, astronomical observations are made by having a telescope pointed to a certain object for a long period of time such that the object will have moved away from the field of view. This requires the telescope to be in motion continuously to track and stay pointed at the object of interest. Factors like these, based on what the telescope is designed to achieve, influence the choice of the mount. An equatorial mount is more complex in design but it offers a great advantage. It has three axes of alignment. One axis is aligned with the celestial pole, and then remains fixed given the axis is not misaligned later on. The other two axes are then used to align it with the object that is to be observed. However, once the telescope is pointed at the object, the telescope can follow the object with motion along a single axis. This allows for an easy tracking of objects for longer periods of time.

The altitude azimuthal or alt az mount has two axes of rotation. Its mechanism is relatively simpler as compared to the equatorial mount, however to track an object, both the axes have to be continuously varied to keep the object in the field of view. This was the mount that was planned for this project. To understand its mechanism, it is helpful to think about the notions of a great circle and a meridian that were explained in the previous chapter. At every point in time, half of the celestial sphere is available for observation. This means the entirety of both the great circle and the meridian are not needed. The azimuthal aspect of the telescope is such that it can be rotated along the entire 360°. For instance, if the telescope is point at the horizon, the azimuthal axis can be varied such that it grazes the entire horizon and comes back to its original position thus having observed an entire great circle. The altitude part has a 90° range. If pointed at the horizon, altitude could be varied to point the telescope all the way up to the zenith. The reason one only needs half the range of a meridian for the altitude axis is that only half the celestial sphere is within the observational limits. It is important to note that, once the alt az telescope is pointed to an object, to find the point on celestial sphere it is pointed to requires not only details on the azimuthal and the altitude angle but also local data on latitude and sidereal time. This extra information is needed precisely due to loss of information due to altitude angle having half the range of a meridian, that is used for celestial positioning. To visually understand the difference between the two categories of mount, the following image obtained from scienceatyoudoorstep.com might help.

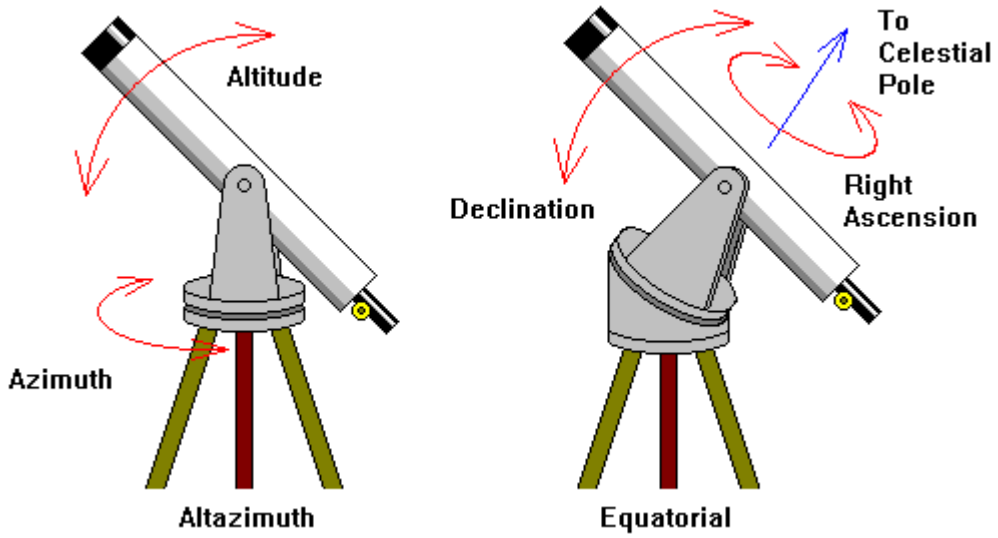


Fig 2.3: Alt Az and Equatorial Mount

With this, the important concepts describing the working of the telescope for this project are covered.

## Chapter 3: Sensors and more

The use of sensors in this project has a very simple purpose. If a telescope is pointed to a certain celestial object, the sensors attached to the telescope should be able to provide data on the angle the telescope makes from the North, and the angle of elevation of the telescope. A board that may comprise of such sensors that could be used for positioning, movement and alignment related observations is called an Inertial Measurement Unit board or an IMU board. This board may have various types of sensors based upon its purpose and sophistication.

For the purposes of this project, an IMU board called the BerryIMU v2 was used. It was interfaced with a Raspberry Pi 3 Model A+, a microcomputer that would take in the raw values from sensors, and convert them into the angles that are needed (mentioned above) and combining them with live local data to be able to provide celestial coordinates of an object under observation.

This chapter is focused on the functioning of the sensors that are used. The complete understanding of their functioning is beyond the scope of this thesis. However, a basic overview of how they function is within the purview. The sensors onboard that are required for the task include an accelerometer, a gyroscope and a magnetometer.

An accelerometer is, as its name suggests, a sensor that can measure acceleration. In general, there is a constant acceleration towards the center of the Earth. If an accelerometer is tilted, the angle of its tilt can be figured out by breaking down the force acting on it in components and using the known values of acceleration

due to gravitational attraction when the accelerometer is aligned properly. Although this data is informative, it may not be accurate. The accelerometer primarily relies on force acting on it. If the sensor is in an accelerated frame of reference, fictitious forces such as centripetal force could be wrongly attributed to acceleration due to gravitation and the values of tilt obtained would then be wrong. This is where the next sensor comes in.

A gyroscope sensor measures the rate of rotation. Integrating this rate can be used to obtain the tilt of the sensor. The gyroscope is not subjected to the errors that would arise from using just the accelerometer readings. One would then rightly question using the accelerometer in the first place. This has to do with running the sensors over an extended period of time. Over time, the gyroscope experiences drift which causes a bias in a certain direction, thus the data would indicate extra tilt in a certain direction. This is where Kalman Filter comes in.

A Kalman Filter is an iterative model to predict data based on past data and predicted model. In oversimplified terms, it takes in the data from accelerometer, makes a prediction based on a model, then takes in the data from the gyroscope, and inputs that in the model and then outputs the data. The iterative approach of correcting the model allows for removal of noise and inconsistencies arising in sensors (such as gyroscope's drift) as the model has been built from data combined from accelerometer and gyroscope over a period of time. The final result is the tilt of the IMU board containing the sensors. Obviously, the sensors can only measure this tilt along one axis and multiple sensors would be needed to have a triple axis tilt

sensitive system. The IMU board used provides for triple axis tilt measurement, however, for the purposes of the project, only one axis needed for the tilt measurement is used to find the angle of elevation of the telescope, i.e. what angle the telescope makes with the horizon. This angle will be referred to as kalmanY (indicating that the axis labelled as the y axis of the IMU board is the axis to which the data corresponds) within the code shown in Appendix A.

The next sensor that is needed is the magnetometer. One of the angles one needs for celestial mapping is the angle from true North. A magnetometer measures the heading from the magnetic North, however, data on local coordinates can be used to correct the heading to obtain the heading with respect to true North. Another problem a magnetometer might run into is that if the sensor is tilted, the heading readings contain huge errors. However, these values can be corrected if the tilt is known and the tilt from the ground, i.e. the angle of elevation of the IMU board attached to the telescope is measured as explained above. By combing the kalmanY values with the obtained heading values, the tilt compensated heading is obtained and referred to as the tiltCompensatedHeading within the code in Appendix A. The two angles, namely the kalmanY and the tiltCompensatedHeading are enough data in terms of what is required from the sensors. Other data is then combined with these two values and processed through an algorithm to find the celestial coordinates as explained in Chapter 6.

## Chapter 4: Optics I- Mirror Making

Mirror making constitutes the most time consuming part of the process of building a telescope. The aim of this part is to start with a flat glass disk, grind it and polish it such that at the end, the disk has a side with a concave spherical/paraboloid profile that is so smooth that the surface roughness (hills and valleys) is of the order of a fraction of the wavelength of light (taken at 550 nm). Before beginning the physical task of grinding and polishing, it is ideal to model the optics of the telescope to ensure the calculations (for optical specifications) made are correct and the whole system works as planned. For the modelling purposes, the software OSLO EDU from Lambda Research Corporation was used. This software has some restrictions on some aspects of modelling, but for the purposes of this project, it suffices.

Before one starts modelling, one needs to have calculated certain parameters for the telescope. In this project, the plan was for an 8 inch[4] mirror[5] with an f-ratio of 8. The f-ratio is the ratio of focal length and the mirror diameter. Hence an 8 inch f 8 mirror has a focal length of 64 inches. It is also important to know the size of the secondary mirror (in terms off its minor axis) that is needed. This can be directly obtained using the modelling software. The software's interface (as shown below) allows to enter the field of view one expects to observe, and accordingly provides with the minor axis value subject to other quantities such as focal length, radius of curvature, mirror diameter, conic constant, etc. Following is the final optical model of

[4] Within this chapter, there will be a lot of different units used. This has to do with the fact that telescope blanks, or telescope specifications conventionally use inches whereas certain experimental apparatus or software that will be used use millimeters or centimeters.
[5] A length written before the mirror is typically the diameter of the mirror.

the telescope barring the eyepiece (as that is decided upon based on magnification and quality considerations at the time of observation).

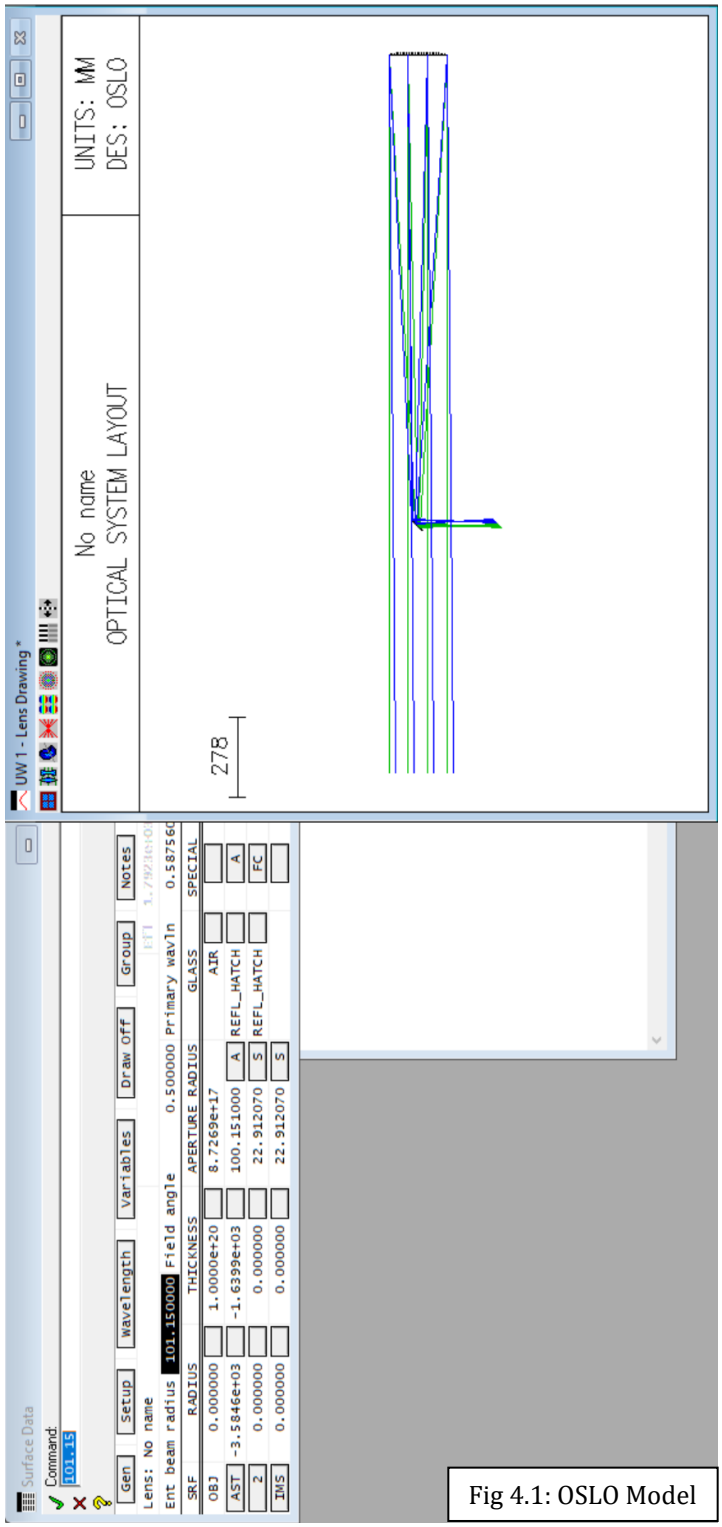


Fig 4.1: OSLO Model

As seen in the image of the optical model above, a number of parameters have to be calculated before one can have a complete model. The model can be used to verify the calculations are correct (because the grinding and polishing is based upon these calculations) and find other optimum quantities based on specific considerations (such as secondary mirror dimensions in the above case). Other thing to note is that within the data, focal length and radius of curvature correspond to f 8.8 instead of f 8. This has to do with decisions one makes during grinding which I will describe in details later on in this chapter.

The next part of the process is grinding. The aim of the grinding process is to get the side chosen to be the reflective side to be turned into a concave spherical surface. An important quantity that the whole process revolves around is the sagitta. This is the maximum depth of the surface as shown below:

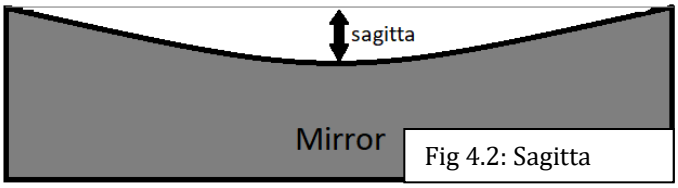


Fig 4.2: Sagitta

To find the targeted sagitta of the mirror, it is useful to remember an important property of a sphere. Every point on a hollow sphere is equidistant from the center of the sphere. Thus the edge of the mirror and the deepest part of the mirror are equidistant from the center of the sphere (which is located at the radius of curvature). Using this property and the Pythagoras' theorem, the sagitta, can be found using the formula below:

$$s = r_c - \sqrt{{r_c}^2 - {r_m}^2}$$

where s is sagitta, $r_c$ is radius of curvature and $r_m$ is radius of mirror. It is important to have consistent system of units while using this formula based on the apparatus one plans to use while making sagitta measurements. For this project, a lab made spherometer (more on this in Chapter 5) is used with units being in mm to an accuracy of 0.01 mm and therefor the calculation is done in mm. By using the formula, sagitta needed is found to be $\left(3251.20 - \sqrt{3251.20^2 - 101.60^2}\right) mm = 1.588\, mm$. However, the sagitta is not measured directly, as the size of the spherometer (due to the type of spherometer designed) has to be taken into consideration. The spherometer's base had a diameter of 6 inches and not 8 inches, hence $r_m$ in the above formula has to be replaced by the radius of the spherometer's base. This gives the following equation: $\left(3251.20 - \sqrt{3251.20^2 - 76.2^2}\right) mm = 0.893\, mm$. This was the targeted value of reading on spherometer that was aimed at when the grinding was completed.

The grinding process requires three parts, the mirror blank, a grinding tool blank and abrasive powder. A grinding tool blank is another glass blank, although other materials could be used for a grinding. The abrasive powder used for grinding glass is generally Silicon Carbide and Aluminum Oxide. Both comes in multiple grit sizes. The higher the grit size, the finer the powder. When the abrasive powder is placed between the mirror blank and the tool blank and the surfaces are moved against one another, silicon carbide, chips away very small bits of glass, and simultaneously breaks down itself. This breaking of glass not only excavates the portion of glass as desired, it also causes fractures to appear and makes the surfaces

very rough and this is the reason one would use finer and finer grits as explained below.

The grinding process can be subdivided into rough grinding and fine grinding. While rough grinding, the aim is to remove as much glass as possible while nearly reaching the targeted depth of sagitta whereas in fine grinding, the aim is to gradually remove the surface roughness caused by rough grinding and simultaneously get the surface to as close as possible to a spherical shape.

The process of rough grinding begins by placing the grinding tool and sprinkling the coarsest abrasive powder with some water to give it a somewhat thin paste like consistency. Then the mirror blank is placed about 30-40% off center above the tool and moved up and down almost along its center with the edges having a 1/3$^{rd}$ of the diameter overhang. The following picture depicts the grinding motion:

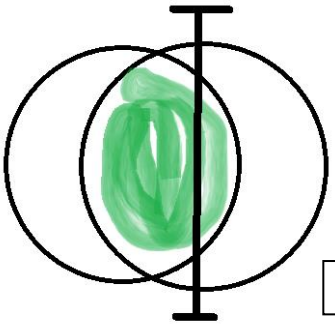

Fig 4.3: Chordal Strokes

This particular type of stroke is known as the chordal stroke. The mirror blank has to be moved along the vertical line between the two horizontal lines. These strokes would have to be completed for a random number of times, say 10, and then the tool would have to be rotated clockwise and the mirror blank would have to be rotated anticlockwise or vice versa and the grinding would continue and so on. After a number of such rounds within a few minutes, the screeching sound of grinding would

subside indicating that the silicon carbide powder has broken down and no new grinding action is taking place. This would be the time to clean up the glass and abrasive residue between the tool and the mirror with water, add some new slurry and carry on. After several rounds, the mirror blank would start showing the concave shape developing in its center whereas a convex profile would be seen on the tool. It is generally here that one would start using the spherometer on the mirror tool to see the depth that has been obtained and carry on. Eventually as around 50 % of the depth is obtained, the center of the mirror should be brought closer and closer to the center of the tool. After a few rounds of grinding and bringing the centers closer, the center of the mirror should be exactly over the center of the tool. The strokes would still have to have 1/3$^{rd}$ of the diameter overhang. These strokes are called the normal strokes.

The normal strokes would be continued until around 80-90 % of the depth is reached with the coarsest abrasive powder. After this, it is time to switch to the next grit size and continue with the normal strokes. The idea from here on is to continue with normal strokes and ensure the surface roughness is reducing. After a few hours with a grit size, it becomes evident that surface roughness has come down uniformly across the entire mirror surface. This is the time to switch to higher grit sizes. Another correction that happens while the normal stroke is performed is that chordal stroke is, albeit faster, a method that creates a non spherical surface. The normal strokes fixes that and returns the mirror surface close to spherical. To test whether the surface is spherical, use the spherometer to measure the depth at the exact center, and given that the spherometer's base is smaller than mirror's diameter, it can be used to test depth at different regions of the mirror. A spherical mirror has exact

depth reading for any part of its surface. After having made the surface almost spherical and having reached the last grit used for rough grinding (typically between 400-600), it is time to switch to fine grinding. The photo below shows the mirror blank after rough grinding:

Fig 4.4: Mirror blank post rough grinding

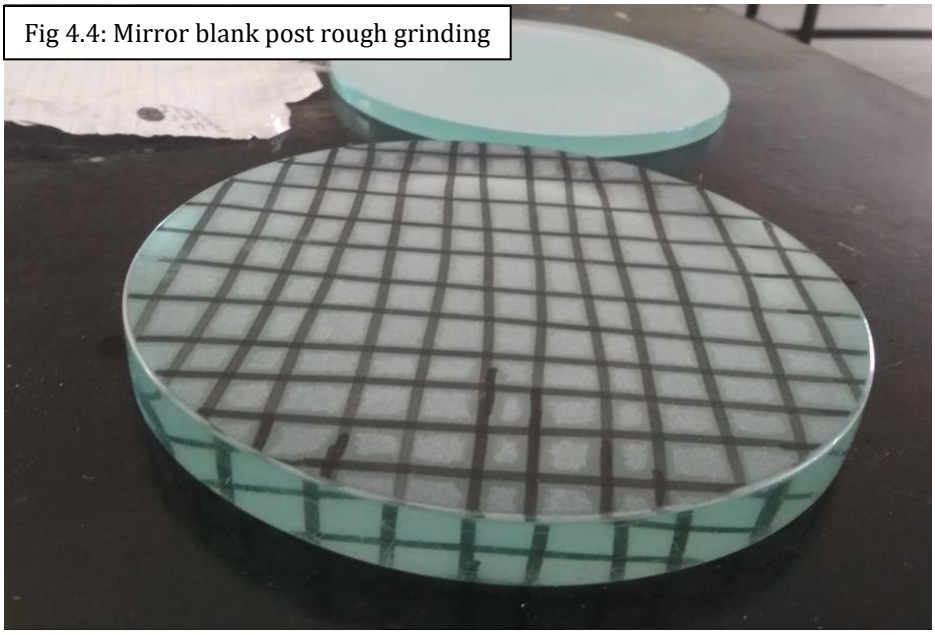

The grid that appears on the glass is drawn using a regular marker. While grinding, the grid starts to wear off. It should be the case that the grid wears of uniformly across the surface. If that is not the case, it indicates ununiform contact between the mirror blank and the tool blank. In that case, grinding should be continued till proper contact is achieved. It is also possible that while trying to make the mirror spherical or completing rough grinding, the sagitta depth overshoots. In this case, the mirror blank should be placed on the bottom and the tool blank on top. The blank on top typically losses more glass in the center whereas the blank at the bottom losses more glass from the edges. It is however possible that the desired sagitta is off by some amount and it would take significant amount of time to get to the target with the grit size that

is currently being used. This was a factor that led to the change in focal ratio of the mirror from f 8 to f 8.8. Having to change to f 8 would have required either too much time with the grit size on hand or having to return to coarse grits and redoing all the work for a lesser amount of time. Therefor, during rough grinding, one should also be prepared to make some decisions that may change the proposed specifications based on the situation at hand.

The procedure for fine grinding is almost similar. This is the time when one typically uses aluminum oxide abrasive powder which is a soft abrasive material. That allows to grind the glass slowly without causing in too many cracks or fractures. One would have to uses 3-4 grit sizes of it typically between 600 to 1000-1200. By this time, grinding has gotten a lot quieter and hence the sound is no longer a guide to when to replace the slurry. However, by this time, the person working on this has developed a sense to be able to tell that the slurry has to be replaced. Eventually, the mirror gets smooth and appears slightly reflective when viewed from an angle. The following is a picture of the mirror blank with just a couple of hours away from being completely fine ground:

Fig 4.5: Mirror blank post fine

Post fine grinding, the process of polishing has to be done. Polishing is done with a polishing compound such as cerium oxide or red rouge. Rouge is generally more readily available, but a very difficult material to work with. The polishing is done with a pitch lap and not the tool that was being used so far. The pitch lap is made by pouring molten tar mixed with some other compound depending on the viscosity one is aiming for (beeswax to make the pitch softer in this case) over the original glass tool or some other rigid base. The mirror is then pressed onto the tar with some polishing compound slurry in between so that the pitch conforms to the mirror's shape perfectly. This conforming to mirror's shape has to be perfect and if it is not the case, it is possible that there are some problems with the pitch that is being used. This was the entire reason the mirror within this project couldn't be completed at the very final stage as is explained in a while. After the pitch lap conforms, grooves/channels are cut into it to allow for flow of air, water and polishing compound. The pitch lap over the grass blank looks as follows:

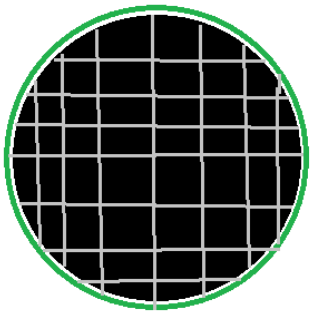

Fig 4.6: Polishing tool/pitch lap over glass blank

Once the pitch lap is made, polishing is done with the same procedure, slurry made using polishing compound and polishing done with normal strokes and

periodic rotation of mirror blank and pitch lap. Over time the glass gets clearer and clearer. To the naked eye, it starts appearing completely clear. At this point one has to start doing the laser test. Although all tests for the mirror are explained in the next chapter, this test is very simple and a very critical part of the polishing process hence it is discussed here. If a 5 mW laser pointer is pointed at the mirror's surface at a roughly 45° angle, some light will pass right through whereas some will scatter off the top surface. What will be noticeable is that after every few hours of polishing, the scattering of light off the top surface will have reduced. The target is to have it be such that no light scatters when this particular test is conducted.

The general time it would take to polish an 8 inch mirror is somewhere between 20-30 hours. Around the 25 hour mark, the scattering of light was near 15-20% of what it initially was. It was assumed that within the next 3 hours or so, polishing would be complete. However, after this stage, no improvement was noticed for hours on. The polishing was done for about 60-70 hours and the scattering of light came just near 10-15 % of the original amount. This had to do with improper pitch lap. It was highlighted above that the pitch lap has to conform perfectly with the mirror. The reason for this will be explained with the aid of the picture below:

Fig 4.7: Imperfectly conformed pitch lap

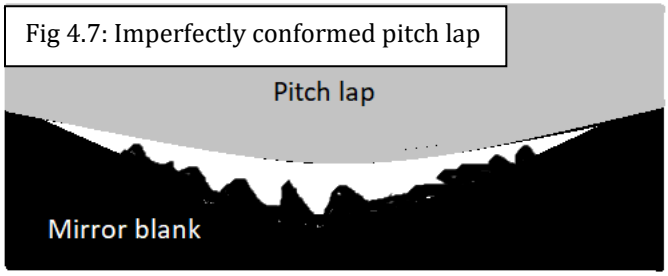

Considering the above image, albeit exaggerated in scales, one sees that if the pitch does not conform properly, it will not be able to remove the bits of glass that cause the roughness. During the polishing, multiple pitch laps (around 15+) were made with different techniques and consistencies and none conformed properly. The fact that the pitch did not conform could be observed given hours of experience was gained while polishing. To have a sense of how every step went as per plan except for polishing, the following table might help which shows the time spent on the 3 processes during the project as compared to average expected time required for the same 3 processes as provided on amateur telescope making forums.

| Process | Time Spent (hours) | Time Expected (hours) |
|---|---|---|
| Rough Grinding | 42 | 30-40 |
| Fine Grinding | 13 | 10 |
| Polishing | 65 | 20-30 |

Table 4.1: Mirror Making Process Time

Noncompletion of polishing meant the mirror could also not be figured, which is when its surface profile is brought to a complete and perfect parabola, although that was not completely necessary anyway, given the high focal ratio of the mirror. With it not being possible to complete the very last 2-3 hours of polishing due to problems with the pitch lap, the mirror could not be sent to be aluminized. The surface roughness of the mirror was such that it may be barely noticeable even after having been aluminized but the light from celestial bodies is limited. It is therefor important that the mirror not only avoids scattering of light due to roughness but also this scattered light would cause flaring of objects thus decreasing the quality of the objects being viewed. The mirror however, was at enough optical quality to be

subjected to the optical tests for a number of characterizations. Had it been possible to complete the polishing, and based on its updated focal ratio of f 8.8 and a targeted maximum field of view of 0.5°, OSLO had shown a secondary mirror of minor axis of 46-47 mm would be needed and hence the final telescope would have been an 8 inch f 8.8 Newtonian Reflector with a 0.5° max FOV.

## Chapter 5: Optics II- Mirror Testing

In this chapter, 4 tests and/or their set ups will be looked at. All the results obtained from the tests described above will be presented in Chapter 7. The first is an explanation on the spherometer that was referred to in the previous chapter. This is followed by explanation and procedures of a Star Test, a Ronchi Wire Test and a Foucault Knife Edge Test. Initially the 3 optical tests were planned to be done in a qualitative manner to ensure every aspect was fine. However, the problem with the completion of the mirror resulted in an extension of the work that had to be done as part of testing. Due to this, the Foucault knife edge test was done very thoroughly and quantitatively to obtain numerical data characterizing the surface profile of the mirror. All the tests explained here were built from scratch within the lab.

The spherometer, as explained in the previous chapter, is used to measure the bulge or depth of a surface. A spherometer in general has to have some fixed point and a moving area of contact. For the purposes of this project, one was constructed such that it had 3 points lying on a circle of 6 inch diameter. A micrometer with a metallic ball at its end was attached at its very center. The 3 points (with a metallic ball each) lying on the edge defined a unique plane. The center ball could move up and down. To calibrate it, the spherometer has to be placed on a completely smooth and flat surface. The center ball attached to micrometer is moved to touch the surface at a single point, without causing the spherometer to shake. The reading at the micrometer at that point is the zero reading. All other readings could be compared

with it to find the difference and thus know the depth of height of the valley or the hill of the surface. Following is the picture of the spherometer constructed:

Fig 5.1: Spherometer

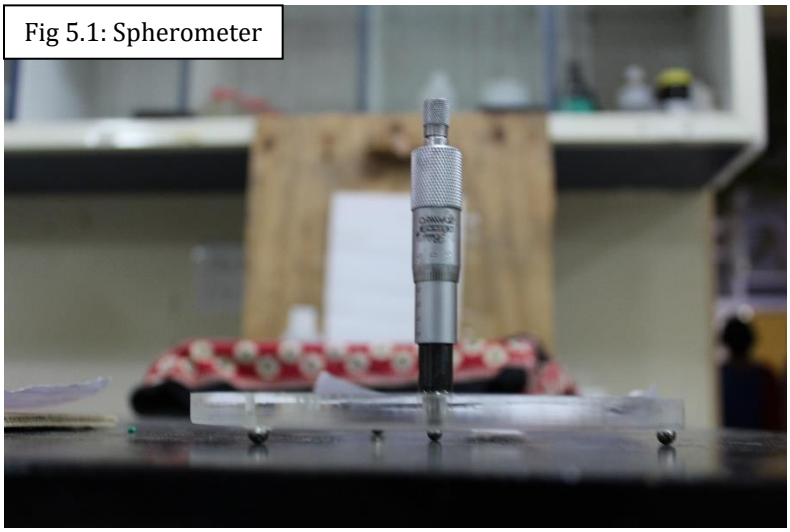

The next part pertaining to this chapter is the star test. This test may be one of the easier ones in principle, however, it requires utmost care with alignment or one would end up thinking there are errors with the mirror, as was the case within this project until corrections were made to the setup (explained below).

The star test would typically require a somewhat complete setup of telescope. The not-yet-aluminized mirror[6] is placed in its regular place within the telescope and the telescope is pointed at a bright star. The image of the star is then viewed through a low focal length eyepiece on 3 different positions, namely inside focus, at focus and out of focus, corresponding to the focal point of the mirror. The patterns observed could be used to verify the image quality that the telescope would deliver once its readied. The alternative to the regular star test setup, is an indoor/artificial star test.

[6] Glass surface typically reflects some light and lets the rest pass through. It is this light that it reflects that is used to perform Star, Ronchi or Foucault test without the need of having the surface aluminized.

This test requires placing the mirror upright and sideways. Tens of meters away from it, a light source with a pinhole in front of it is placed. This point source acts as an artificial star. The pattern is observed with an eyepiece at the focal length. The whole process requires taking care of a number of aspects. The first is to ensure the mirror is placed in a stable and sturdy position and the setup allows for fine tuning its tilt to ensure the light from the source is nearly parallel to the optical axis. This is done by having a proper support structure for mirror as shown below:

Fig 5.2: Mirror Support Structure

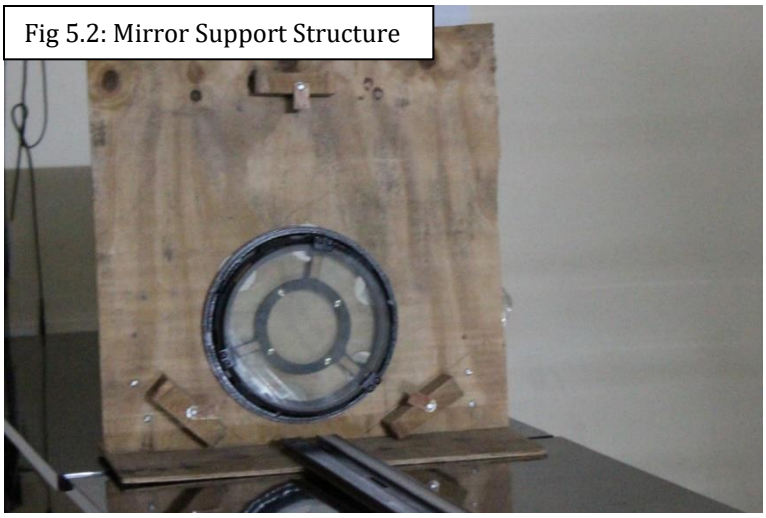

This structure was built from scratch for the very purpose of mirror testing. It has a well supported base and the actual mirror cell that is used in telescope construction is mounted to it to allow for not only safe mounting of the mirror but also fine tuning the direction of the mirror for the purposes of alignment. This structure suffices for the Star, Ronchi and Foucault test.

The second aspect to lookout for in the star test is the alignment. Its importance lies in the way reflection takes place. The point source essentially emits semi spherical waves. If the direction of propagation of the wave front isn't parallel to the optical axis (let it be z axis), the wave front would have some component in the

x-y plane. However, the component along the x axis may differ from the component along the y axis. When the observer views the star test patterns from inside the focus or outside the focus, this difference in x and y component makes an observable difference. The difference however is such that the observer would mistakenly think that the mirror has astigmatism. An astigmatic mirror has different radii of curvature along different directions. Refer to figure 2.2 where it was explained that a single curve could be rotated around the z axis. Assume that the curve, while rotating around the z axis, evolved such that the surface generated has a symmetry only for all curve segments that are separated by 180°. Such a mirror surface would have different radii of curvature and therefor different focal lengths along different directions. In the case of a star test, improper alignment causes patterns indicating astigmatism corresponding to two directions, as one would expect, given the x and y component arguments made above.

To align a star test in a regular star test is somewhat easier that the artificial star test. In the regular star test, a secondary mirror is present in its position and the light the secondary mirror blocks from reaching the primary mirror is relatively less. However, within the indoor star test setup, using a secondary mirror would pose its own challenges in terms of alignment without the telescope structure guiding its positioning. Hence an easier way to perform it is to directly place the eyepiece at the focal length. This however causes the observer's head to obstruct much more light than a secondary mirror would. It then becomes imperative to have the point source emitting light that is very slightly off axis such that observed patterns do not show astigmatic properties.

The next two tests have a very similar setup with just one key difference. The following is an image is the setup:

Fig 5.3: Mirror Test Setup

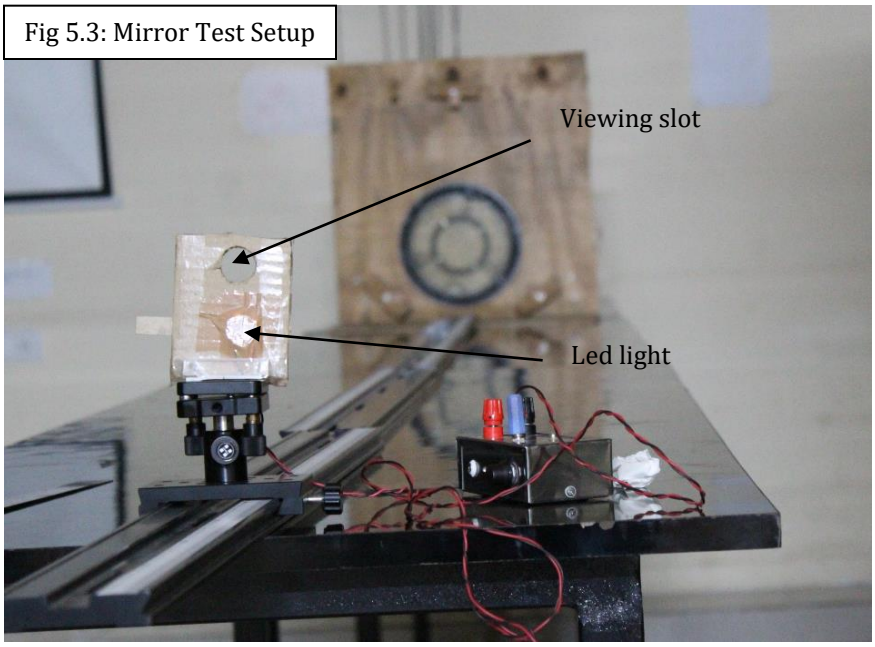


This setup has a light point source placed at the radius of curvature of the mirror. The mirror is tilted such that the beam of light is very nearly parallel to the optical axis. The slight tilt is to ensure that the returning beam is aimed at the viewing slot. At the viewing slot, there is a Ronchi Grating or a Knife/Blade Edge attached. Each of these tests can be performed at varying levels of complexity. The setup shown above was designed for basic qualitative tests. The following image explains the difference between the two tests within the viewing slow:

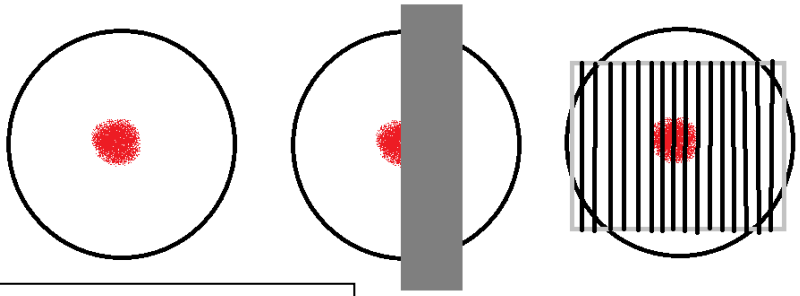

Fig 5.4: Viewing slot versions

The first diagram shows how the viewing slot looks without any other object. The second diagram shows the viewing slot where a knife edge cuts the image. The third diagram shows a Ronchi grating through which the image is observed.

The Ronchi wire test was performed at the level planned. Its sole purpose was to see whether the mirror had a conic constant of zero or lesser than zero. The results and methods of interpretations are available in Chapter 7.

The Foucault knife edge test was initially done at a very basic qualitative level, however, it was later decided to do a thorough quantitative test to obtain a better analysis of the surface profile of the mirror. This quantitative analysis requires the use of properties of a spherical surface to characterize various surfaces, including ones that aren't spherical. The setup however, requires some modification to allow for the necessary data to be collected. The modified setup is such that the source of light and the viewing slot are separate. The source of light and the viewing slot are aligned such that their distance from the mirror is identical and the light focuses perfectly. This distance is the exact radius of curvature. There are some difficulties in measuring this distance accurately, but nevertheless it isn't difficult to find this point and align the components of the setup with respect to the radius of curvature. Next, the viewing slot had to be attached to a translational slide with a very sensitive micrometer with an accuracy of 0.005 mm for fine movements along the optical axis.

The principle behind the test has to do with how spherical mirrors reflect. A point source of light originating from the radius of curvature of the mirror and reflecting off it will on focus right back at the radius of curvature. If a blade edge is

placed to cut the beam from one side, for instance the right side, multiple possibilities exist. If the blade is placed inside the radius of curvature, the mirror will appear to be in dark on the right side, and if the blade is outside the radius of curvature, the mirror will appear to be in dark on the left side as the image is inverted outside the focus. At the focus, the entire mirror appears in dark as the focus point is just that, a point. The blade is unable to cause just a single part of the mirror to be in dark.

Consider a concave surface. If it is divided into zones, such that there is a central circular zone and concentric ring zones outside of it. Each of these zones is such that it has the same area. Given a general concave mirror is not spherical, it would be right to assume that different zones have different radii of curvature. If the knife edge test is conducted on such a surface, the readings could be taken for the radius of curvature of each of the different zones. The individual readings need not be the complete radii of curvature of each zone but rather the difference in radius of curvature with respect to the central zone. The following two images from the test show two different zones that have been darkened using the blade edge:

Fig 5.5: Central Zone

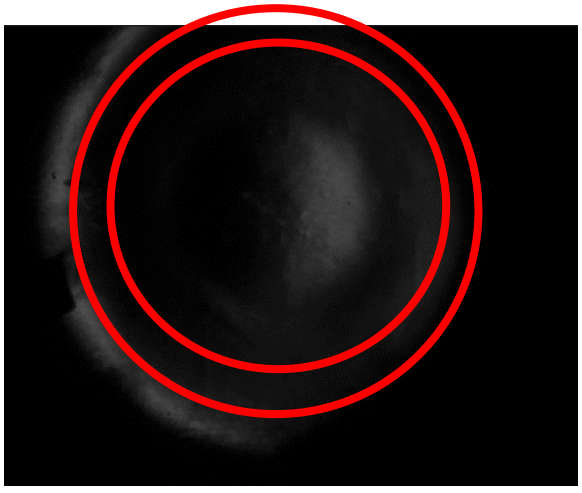

Fig 5.6: Second Outermost Zone

The above pictures lack clarity due to difficulty in taking such pictures. The pictures were captured using a camera mounted on a tripod and the small viewing area of the pattern (as the image is taken very near its point of focus) makes it difficult to align the camera to capture maximum light for greater clarity. Nevertheless, taking readings of differences in radii of curvature through an eye based observation and then analyzing the data through a dedicated software can provide valuable information on the surface profile of the mirror. The quantities obtained include the exact conic constant of the mirror, the amount of glass required to be removed from different zones to change the conic constant to the desired conic constant (such as -1 for a paraboloid), amount of light that reflects back from the surface to the desired point of focus and so on. The important aspects of the analyzed data are presented in Chapter 7. This concludes the explanation on the main testing methods used for the purposes of this project.

## Chapter 6: Sky Map System

In Chapter 1, the concept of celestial coordinates was thoroughly developed. In Chapter 3, it was explained how the sensors work and the quantities of interest are the heading (magnetic heading) and the angle of elevation (kalmanY). It should also be noted that in Chapter 2, within the explanation of the alt az mount, it was explained that 2 degrees of freedom are required to uniquely identify a point on a semi sphere where one axis has a range of 0° to 360° and the other axis has a range of 0 to 90°. The implementation of celestial coordinate mapping is based on a system very similar to the principle of the alt az mount.[7] The heading ranges between 0° to 360° and the angle of elevation ranges between 0 to 90°.

Within this chapter, the entire process from taking the readings of heading and angle of elevation to arriving at the RA and Dec of an object will be explained. The Python program that was written to perform this task is shown in the appendix.

The heading that has been obtained from the IMU board, is the tilt compensated magnetic heading. However, the celestial coordinates system have poles that correspond to the true/geographic poles, and not the magnetic poles. Therefor the magnetic heading obtained is corrected by addition or subtraction (based on the observer's location) of the magnetic declination. This provides the true heading.[8] The angle of elevation is subtracted from 90° which gives the angle from

[7] It should be noted that the similarity between the sky map system and the idea behind the alt az mount system does not restrict the usage of the sky map system to a particular mount. The similarity is highlighted to merely make the reader understand the principle of identifying points on a semi sphere, which was explained while the alt az mounts were introduced.
[8] From here onwards, heading is with respect to true North.

the zenith.[9] The other two quantities of interest are the local latitude and the local sidereal time. Local latitude is constant but local sidereal time changes continuously hence within the program, a library called the PyEphem is used to provide with the current local sidereal time.

Before going into the algorithm used to calculate the RA and Dec, a few points should be noted:

i. Local latitude is equal to the Dec of zenith
ii. Local sidereal time is equal to the RA of the zenith
iii. Heading is the azimuthal angle from the North and the North Celestial Pole
iv. Zenith Angle can be interpreted as the angle between the observer's location and the location at which the object being observed is at the zenith

To proceed, some numbers will be taken to make the explanation easier to grasp. Consider that the local latitude is 20° N and local sidereal time is 12:00:00, i.e. observations were made when the coordinates at zenith were Dec = 20° and RA = 12:00:00. There are four special cases that make calculations easier so they can be looked at first. They include heading = 0°, 90°, 180° and 270°.

Special case 1: At 0° heading, assume two cases, one is where zenith angle is 40° and the other where the zenith angle is 75°. For the first case, we have our telescope pointed at an object such that heading reads 0° and zenith angle reads 40°, this celestial object lies on the same meridian as the zenith hence it's celestial

[9] This quantity will here onwards be referred to as the zenith angle.

coordinates are Dec = 20° + 40° = 60° and RA = 12:00:00. For the second object, its meridian is separated from the meridian at zenith by 12 hours. This is because this object is zenith to a location on Earth, that is on the other side of the North Pole corresponding to the defined observer in the example. Hence for this object, the Dec = 90° - (20° + 75° - 90°) = 85 ° and RA = 00:00:00.

Special case 2: The second special case is where the heading is 180°. Here the opposite of first case has to be done, i.e. the value of zenith angle has to be subtracted. For instance, an object for which heading reads 180° and zenith angle reads 33°, the Dec = 20° - 33° = -13° and the RA = 12:00:00.

Special case 3: For this case, the heading reads 90° and the zenith angle reads 60°. This celestial body has Dec that equals with the latitude of the observer. The RA can be calculated by adding 60° to 12:00:00 i.e. 04:00:00 + 12:00:00 = 16:00:00. This indicates the celestial coordinates of the object are Dec = 20° and RA = 16:00:00.

Special case 4: This case corresponds to the heading reading 270°. Here the opposite of case 3 has to be done, i.e. the zenith angle has to be subtracted from the sidereal time hence a celestial body for which heading reads 270° and zenith angle reads 60° corresponds to an object located at Dec = 20° and RA = 08:00:00.

The 4 special cases were in some sense, trivial, for only one of the values, Dec or RA was different from the coordinates of the zenith. Dealing with objects not within these special cases can be made simpler by breaking down the sky into quadrants. Consider the position mentioned above with Dec = 20° and RA = 12:00:00 as the origin. The declination line of 20° is the horizontal axis and the RA line of 12:00:00 is

the vertical axis. The algorithm can be broken into steps after the considerations stated above are made:

i. Calculate the angle between the horizontal line (that corresponds to the quadrant) and the heading. This, very simply means, for heading between 0° to 90°, calculate 90° - heading, for heading between 90° to 180°, calculate heading - 90°, for heading between 180° to 270°, calculate 270° - heading and for heading between 270° and 0°, calculate heading - 270°. From here onwards, this angle will be referred to as θ.

ii. Calculate the sin(θ) value and the cos(θ) value.

iii. For Dec, if the object lies is 1st or 2nd quadrant, i.e. the heading lies between 0° to 90° or between 270° to 0°, add the value of sin(θ) * zenith angle to Dec of zenith. If the object lies in the 3rd or 4th quadrant, i.e. the heading lies between 90° to 180° or between 180° to 270°, subtract the value of sin(θ) * zenith angle from the Dec of zenith. This value is equal to the Dec of the celestial object.

iv. For RA, convert the cos(θ) * zenith angle value from degrees to hour angle format, i.e. HH:MM:SS, if the object lies in the 1st or 4th quadrant, add the hour angle value obtained above to RA of zenith, and if the object lies in the 2nd or 3rd quadrant, subtract the hour angle value obtained above from the RA of zenith. This final value corresponds to the RA of the celestial object.

One other aspect to make note of while performing these calculations is to note that it is possible for the values obtained of Dec to be more than 90° or less than -90°.

An example of such a scenario occurring is provided in special case 1 for the celestial body that has a zenith angle of 75°. In such cases, the method to obtain the correct Dec and RA is as follows:

i. For RA, take the RA that has an hour angle difference of 12:00:00 from the RA at zenith.
ii. For Dec, if the Dec exceeds 90°, subtract the obtained value of Dec from 180° to find the actual value of Dec.
iii. For Dec, if the value if less than -90°, subtract the obtained value of Dec from -180° to find the actual value of Dec.

The other possibility is that the RA is calculated to be below 00:00:00 or above 24:00:00.[10] In such a case, the method to obtain the Dec and RA is as follows:

i. Dec is obtained by method described above.
ii. If RA is below 00:00:00, add the obtained value of RA from 24:00:00 to find the actual RA.
iii. If RA is above 24:00:00, subtract 24:00:00 from the obtained value of RA to find the actual value of RA.

This wraps up the complete explanation on how the readings obtained from the IMU board are combined with observer specific data to find the celestial coordinates of the object at which the IMU board is pointed. The complete Python code is included in the Appendix A.

[10] 00:00:00 and 24:00:00 refer the to exact same RA.

## Chapter 7: Optical Testing Results

One of the most primary tests of a mirror is one that is used to calculate its radius of curvature. In Chapter 4, the equation $s = r_c - \sqrt{{r_c}^2 - {r_m}^2}$ was shown as a way to calculate the targeted sagitta while grinding. During the final stages of polishing, this equation can be rearranged to find $r_c$ by measuring the value of s and using the known value of $r_m$. This is done as the grinding and polishing processes do not always lead to the exact sagitta desired and the result may cause for radius of curvature to be slightly off of the desired radius of curvature. This is not a problem, however it is important for the final radius of curvature to be known. The measured value of sagitta during the final stages of polishing was 0.81 mm. Calculation of the radius of curvature and subsequently the f ratio shows the mirror has an f number of 8.8.

The star test had initially displayed signs of astigmatism in the mirror. The nature of the star test was such that taking photographs using a regular sized camera is not possible (as the camera would obstruct light reaching the mirror). Therefor, the observations were recorded through hand drawings. The following are the results drawn that showed astigmatism:

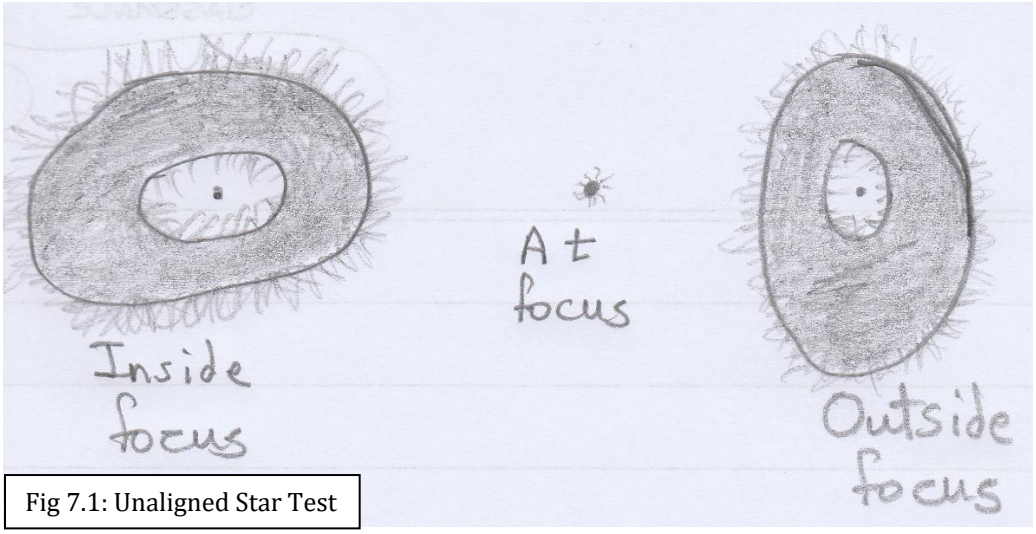


Fig 7.1: Unaligned Star Test

The setup of the test was than adjusted so as to perfectly align the light source with the mirror (as explained in Chapter 5). The following were the results:

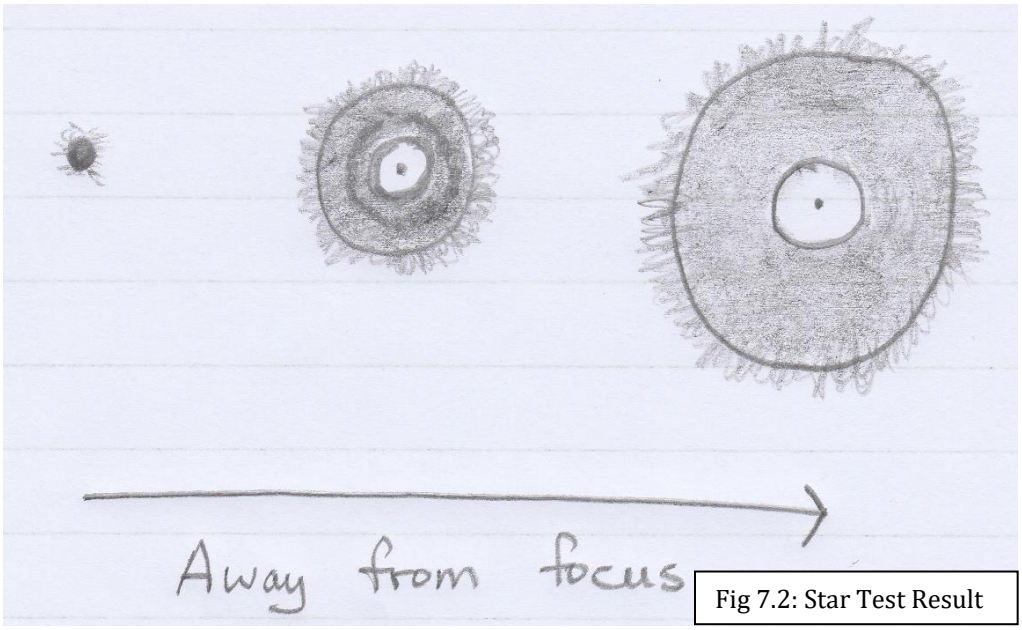


Fig 7.2: Star Test Result

The results cam be understood as follows: The unaligned setup shows elliptical rings as opposed to circular. This happens when the radius of curvature along one axis is shorter than the other axis thus elongating the image along one axis while nearer and vice versa. This indicates astigmatism. However, this was not the case as results were merely a result of improper alignment. After the setup was aligned properly, the

results obtained were as shown in Fig 7.2. This is very similar to a perfect star test as described in an amateur astronomy website by Mel Bartels as shown below:

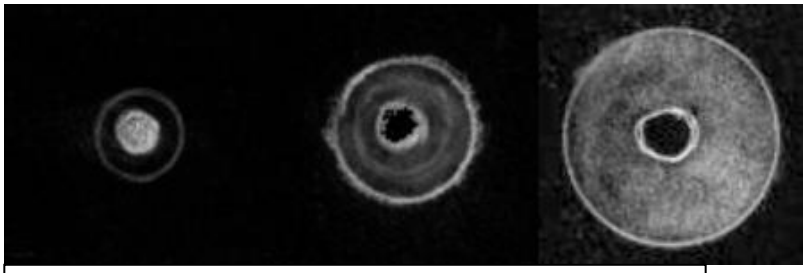

Fig 7.3: Perfect Star Test as shown on bbastrodesigns.com

There is one key difference in this perfect star test picture and the results from the Star Test shown above. In Fig 7.1 and 7.2, there is flaring observed on the edges of the rings. This is simply due to the fact that star test has to be performed after the temperature of the mirror completely equilibrates with the room temperature. While the mirror is hand held and placed into the setup, its temperature increases significantly which causes convective air flow during test distorting the image with flares. This demonstrates the fact that the test is a very sensitive one. Apart from the flaring, the Fig 7.2 shows the mirror is reasonably close to being a perfect telescope mirror in terms of surface profile. It is important to note that at longer focal lengths, one could get away with the conic constant being significantly different and still get decent results. Therefor, this result indicates that the mirror's surface profile would yield good images and does not indicate whether the surface is a nearly perfect parabola or sphere or else.

The next test is the Ronchi Wire test. This test was done in a very simplified way. The purpose was to get a sense of the conic constant of the mirror's surface. An

indicative result of the Ronchi test for different conic constants is shown on the telescope-optics.net website, as shown below:

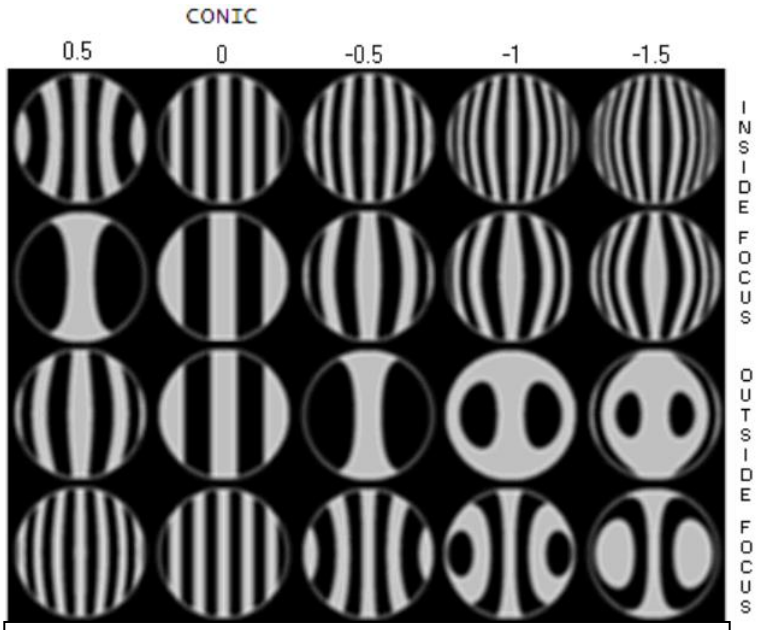


Fig 7.4: Ronchi test results as shown on telescope-optics.net

The observation made using the Ronchi test performed is shown below. The image quality of the results is not great, however the left sides of the images provide a decent outline of the curvature of the lines observed.

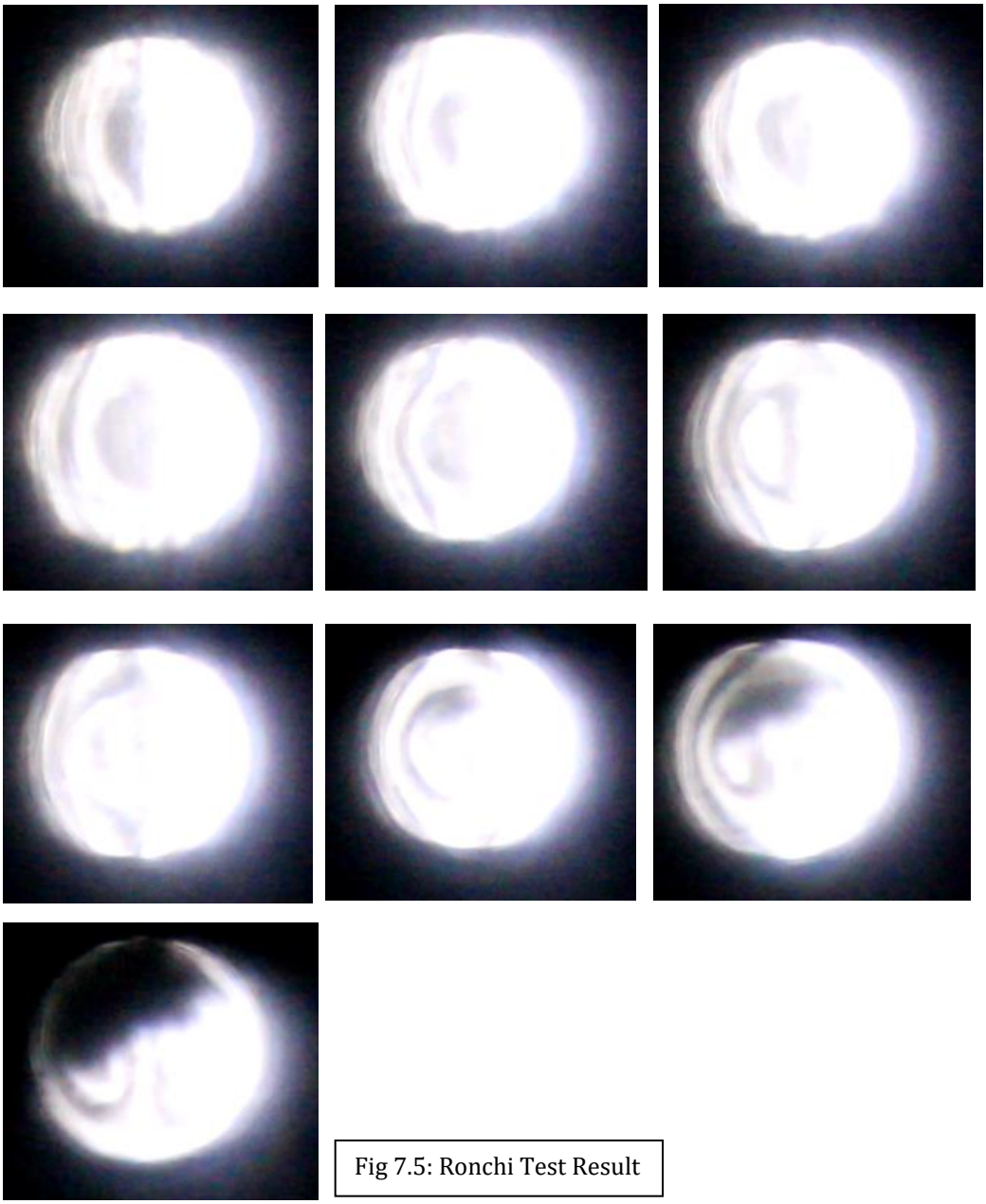

Fig 7.5: Ronchi Test Result

The images are observations made from inside of the radius of the curvature to near the radius of the curvature and finally outside the radius of the curvature. The results were not analyzed quantitatively hence an exact conic constant can not be deduced, however it is safe to conclude that the surface profile lies somewhere in the paraboloid through hyperboloid range.

The final test results to go through are of the Foucault Knife Edge test. This test was the most thorough of all the tests performed. It was performed using setup as shown in Fig 5.3, however the setup was modified to be more sophisticated. The light source was separated from the knife edge to allow for independent movement of the knife edge. The light source and the knife edge were aligned to ensure a few points:

i) the distance between the light source and the knife edge was equal when the reflected light focused on the knife edge

ii) the light source and the knife edge were mounted over a jack to ensure the light source and the knife blade were at the level of the center of the mirror

iii) the knife edge bisected the reflected light at the center, and the axis of movement of the knife edge was parallel to the optical axis

The knife edge's movement along the optical axis was controlled by a translational slide after the knife edge was placed at the radius of curvature of the mirror. It is this movement that would allow for nulling of the zones. 5 zones were designated such that each of them encompasses equal area. The following table displays the boundaries of zones with respect to distance from the center of the mirror:

| Zone | Inner Mask Radius | Outer Mask Radius | Effective Mask Radius |
|---|---|---|---|
| 1 | 0 | 45.437 | 27.424 |
| 2 | 45.437 | 64.257 | 55.248 |
| 3 | 64.257 | 78.699 | 71.660 |
| 4 | 78.699 | 90.874 | 84.896 |
| 5 | 90.874 | 101.6 | 96.312 |

Table 7.1: Foucault knife edge test zones

The test also requires the use of an Everest pin stick or a Coulder mask to distinguish between zones while performing the test. For this test, a paper strip was marked with the distances of the boundary lines as specified in the Table 7.1, and at each boundary line a stick was taped such that it stuck above the paper tape. This allowed for zonal boundaries to be clearly marked with small stick shadows on an otherwise completely lit mirror surface. The Foucault knife edge test was then performed and the distance moved on the translational slide to null each of the zones was recorded. The data was that analyzed using FigureXP, a Foucault test data reduction software. The following is the data that was recorded versus the data that is expected of a mirror that is a perfect paraboloid.

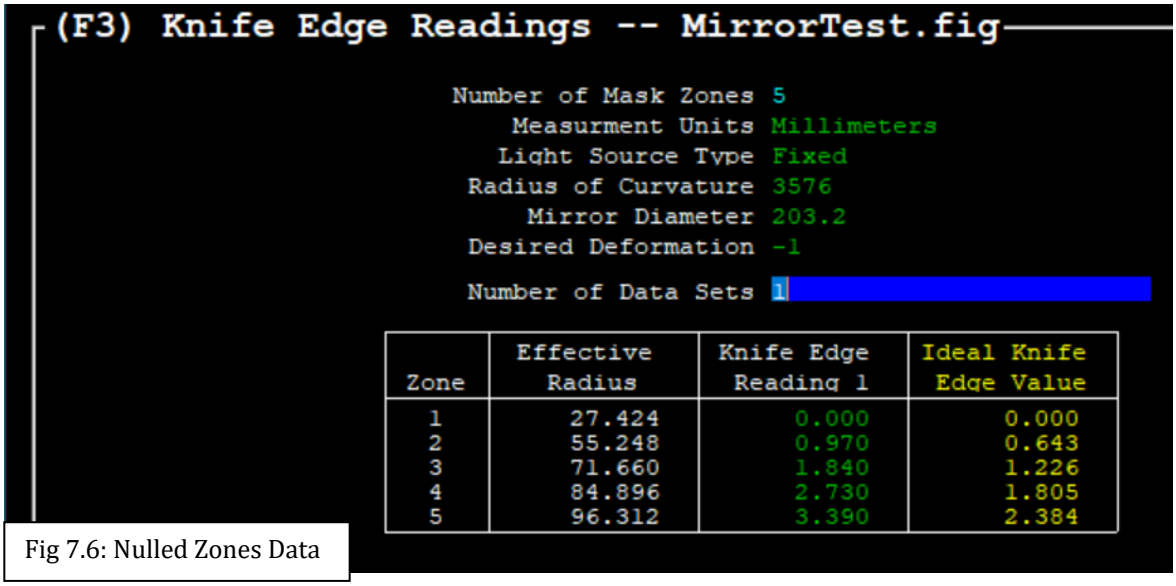


| Zone | Effective Radius | Knife Edge Reading 1 | Ideal Knife Edge Value |
|---|---|---|---|
| 1 | 27.424 | 0.000 | 0.000 |
| 2 | 55.248 | 0.970 | 0.643 |
| 3 | 71.660 | 1.840 | 1.226 |
| 4 | 84.896 | 2.730 | 1.805 |
| 5 | 96.312 | 3.390 | 2.384 |

Fig 7.6: Nulled Zones Data

The following is the surface error analysis obtained:

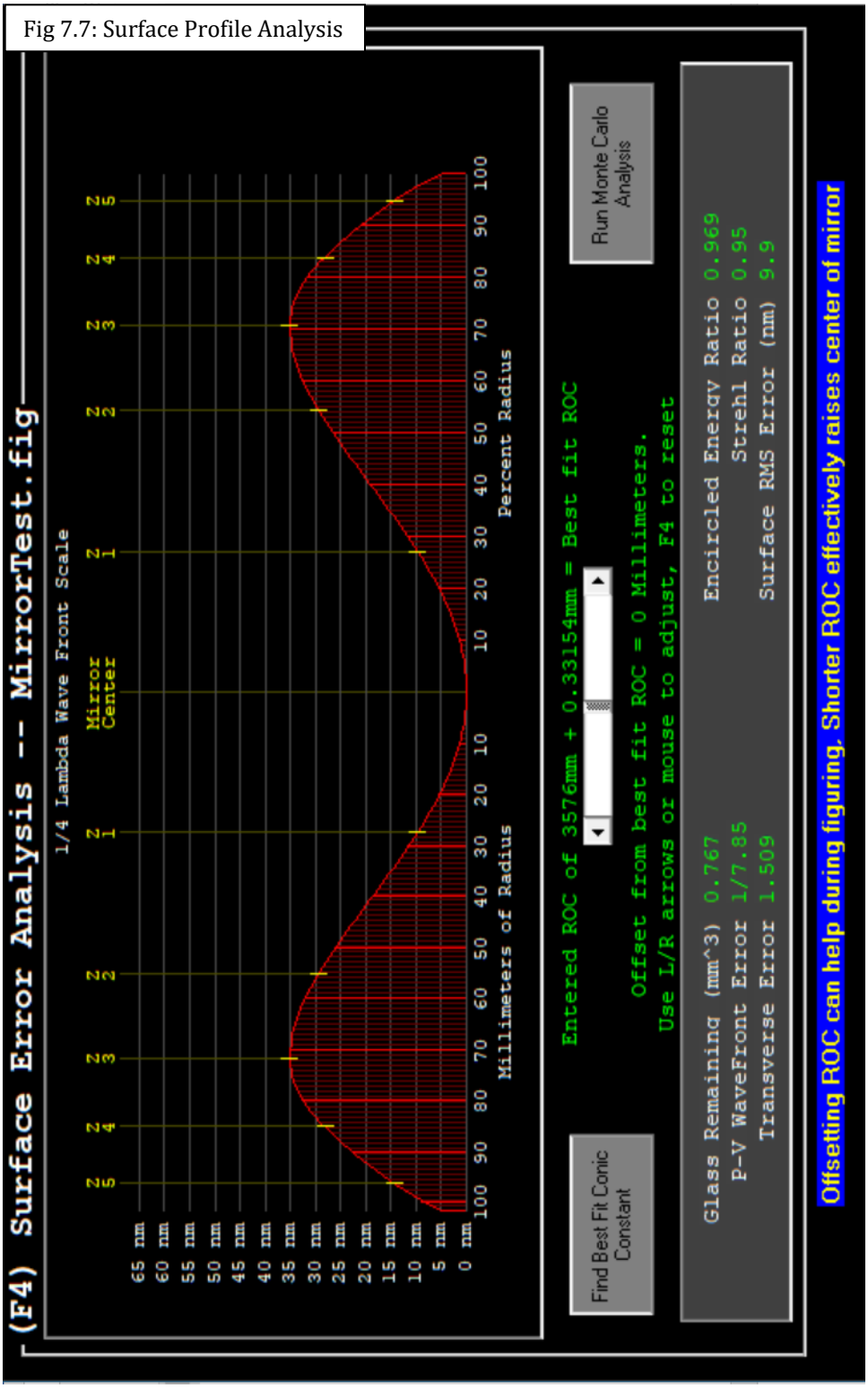


Fig 7.7: Surface Profile Analysis

The conic constant of the mirror based on the test is as shown below:

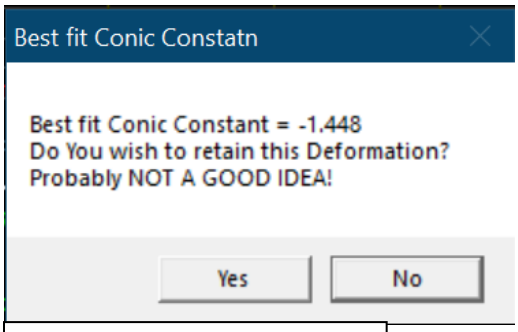


Fig 7.8: Mirror Conic Constant

The first aspect to analyze from the plot above is the difference between the perfect mirror surface and the real mirror surface. It is useful to note that the hills on the graph do no mean that the surface of the mirror has these hills corresponding to about 35 nm. It indicates the difference between the ideal paraboloid surface given the radius of curvature and the surface which has been tested. It is most probably the case that the surface of the mirror actually has a 35 nm valley as compared to that of the perfect paraboloid, given that the conic constant of the mirror lies in the hyperboloid range. This confirms two observations made earlier, one is that made while performing the Ronchi test of the conic constant of the mirror, the second being that problems were consistently observed while making the pitch lap that were such that the pitch lap did not conform perfectly at the center of the mirror. This shows in the analysis above as regions of the mirror outside the mirror are deeper than the center. The other quantity of interest is the Strehl Ratio, which is a number characterizing the quality of the image that would form. At 0.95, it is much higher than what is typically required of a telescope mirror which is 0.80. This concludes the analysis of the mirror and comments on the results of optical testing are included in the Conclusion section of the thesis.

## Chapter 8: Star Catalogue and Sky Map

The celestial bodies mapping was performed in the following way:

i) the data on celestial coordinates was collected for a few seconds for every object

ii) the python script that outputs the value of RA and Dec does so every 0.03s

iii) the data points were saved in .csv files

iv) the data was averaged to output the final values of RA and Dec (this was necessary as the data contained enormous noise)

v) the final average values of RA and Dec were noted for every object and compared to the data available on the planetarium software Stellarium

The following page contains the final data for 108 stars for which data was obtained and analyzed. The measured values for all the celestial objects, of both the quantities, RA and Dec, were found to be correct to within a degree. A sky map was created based on this data which follows the data table.

Table 8.1: Sky Map Data

| Star Name | Stellarium Data | | Collected Data | | Star Name | Stellarium Data | | Collected Data | | Star Name | Stellarium Data | | Collected Data | |
|---|---|---|---|---|---|---|---|---|---|---|---|---|---|---|
| | RA | Dec | RA | Dec | | RA | Dec | RA | Dec | | RA | Dec | RA | Dec |
| Achernar | 1:38:28 | -57.132 | 1:39:37 | -57.415 | Cebalrai | 17:44:29 | 4.56 | 17:46:02 | 4.106 | Muphrid | 13:55:40 | 18.295 | 13:54:42 | 18.445 |
| Acrab | 16:06:38 | -19.86 | 16:07:27 | -19.607 | Cursa | 5:08:52 | -5.061 | 5:09:54 | -4.816 | Naos | 8:04:18 | -40.062 | 8:05:27 | -40.317 |
| Adhara | 6:59:26 | -29.001 | 6:58:34 | -28.775 | Deneb | 20:42:08 | 45.355 | 20:43:21 | 45.632 | Navi | 0:57:56 | 60.825 | 0:58:34 | 61.035 |
| Al Zara | 7:03:53 | -23.864 | 7:03:40 | -24.001 | Denebola | 11:50:06 | 14.456 | 11:50:44 | 14.396 | Nihal | 5:29:06 | -20.744 | 5:27:44 | -21.009 |
| Alcyone | 3:48:43 | 24.167 | 3:48:00 | 24.446 | Diphda | 0:44:37 | -17.873 | 0:43:12 | -17.599 | Nu Pup | 6:38:22 | -43.215 | 6:39:22 | -43.587 |
| Aldebaran | 4:37:06 | 16.549 | 4:36:02 | 16.957 | Dschubba | 16:01:33 | -22.679 | 16:00:18 | -22.996 | Phact | 5:40:22 | -34.064 | 5:39:01 | -34.144 |
| Algenib | 0:14:18 | 15.298 | 0:14:46 | 15.045 | Dubhe | 11:04:59 | 61.639 | 11:05:41 | 61.319 | Phecda | 11:54:52 | 53.582 | 11:55:24 | 53.229 |
| Algieba | 10:21:06 | 19.735 | 10:20:25 | 19.344 | Electra | 3:46:06 | 24.176 | 3:45:14 | 24.442 | Pi Pup | 7:17:51 | -37.135 | 7:18:51 | -37.486 |
| Algol | 3:09:31 | 41.033 | 3:09:02 | 40.733 | Elnath | 5:27:36 | 28.622 | 5:29:17 | 28.164 | Polaris | 2:57:28 | 89.348 | 2:59:21 | 89.211 |
| Alhena | 6:38:54 | 16.379 | 6:37:57 | 16.647 | Eltanin | 17:57:05 | 51.487 | 17:55:50 | 51.705 | Pollux | 7:46:32 | 27.974 | 7:47:17 | 27.525 |
| Alioth | 12:54:56 | 55.848 | 12:54:13 | 56.166 | Enif | 21:45:12 | 9.97 | 21:44:51 | 10.19 | Procyon | 7:40:21 | 5.171 | 7:39:08 | 5.236 |
| Aljanah | 20:47:02 | 34.048 | 20:47:59 | 33.808 | Fomalhaut | 22:58:47 | -29.512 | 22:58:07 | -29.637 | Rasalhague | 17:35:52 | 12.547 | 17:35:17 | 12.188 |
| Alkaid | 13:48:21 | 49.21 | 13:47:46 | 49.309 | Furud | 6:21:06 | -30.073 | 6:19:54 | -30.488 | Regor | 8:10:09 | -47.397 | 8:10:49 | -47.615 |
| Almach | 2:05:10 | 42.428 | 2:05:16 | 42.778 | Gienah | 12:16:52 | -17.656 | 12:14:45 | -17.894 | Regulus | 10:09:26 | 11.867 | 10:08:46 | 12.006 |
| Alnilam | 5:37:15 | -1.19 | 5:37:08 | -1.196 | Gomeisa | 7:28:16 | 8.246 | 7:28:55 | 7.978 | Rigel | 5:15:30 | -8.18 | 5:15:45 | -8.072 |
| Alnitak | 5:41:48 | -1.933 | 5:41:24 | -1.78 | Hamal | 2:08:20 | 23.559 | 2:09:14 | 23.409 | Sadr | 20:22:57 | 40.322 | 20:20:56 | 40.022 |
| Alphard | 9:28:36 | -8.749 | 9:26:50 | -8.168 | Hassaleh | 4:58:20 | 33.196 | 4:59:08 | 33.064 | Saik | 16:38:16 | -10.606 | 16:39:13 | -10.249 |
| Alphecca | 15:35:33 | 26.646 | 15:36:30 | 26.204 | Hatysa | 5:36:26 | -5.897 | 5:37:22 | -5.446 | Saiph | 5:48:42 | -9.664 | 5:48:50 | -9.904 |
| Alpheratz | 0:09:27 | 29.204 | 0:09:22 | 28.492 | Hydor | 22:53:41 | -7.469 | 22:54:14 | -7.741 | Sargas | 17:38:46 | -43.008 | 17:37:43 | -43.134 |
| Altair | 19:51:47 | 8.924 | 19:52:50 | 8.52 | Izar | 14:45:53 | 26.987 | 14:45:17 | 27.071 | Scheat | 23:04:45 | 28.192 | 23:04:15 | 27.907 |
| Aludra | 7:24:54 | -29.344 | 7:23:20 | -28.998 | Kaus Australis | 18:25:32 | -34.372 | 18:23:52 | -34.163 | Shaula | 17:34:58 | -37.116 | 17:34:00 | -37.486 |
| Alzirr | 6:46:27 | 12.871 | 6:47:30 | 12.378 | Kochab | 14:50:40 | 74.07 | 14:50:19 | 74.57 | Shedar | 0:41:40 | 56.647 | 0:42:47 | 56.201 |
| Ankaa | 0:27:18 | -42.194 | 0:29:49 | -41.576 | Kraz | 12:35:28 | -23.51 | 12:36:10 | -23.271 | Sigma Pup | 7:29:52 | -43.343 | 7:30:38 | -43.013 |
| Antares | 16:30:40 | -26.476 | 16:30:24 | -26.785 | Larawag | 16:51:30 | -34.329 | 16:52:07 | -34.578 | Sirius | 6:46:02 | -16.745 | 6:45:40 | -16.572 |
| Arcturus | 14:16:36 | 19.074 | 14:16:47 | 19.929 | Mahasim | 6:01:07 | 37.212 | 6:01:40 | 37.254 | Spica | 13:26:15 | -11.266 | 13:26:06 | -11.196 |
| Arneb | 5:33:38 | -17.808 | 5:34:31 | -17.645 | Markab | 23:05:47 | 15.317 | 23:05:03 | 15.648 | Suhail | 9:08:44 | -43.515 | 9:10:15 | -43.144 |
| Athebyne | 16:24:16 | 61.467 | 16:26:48 | 61.569 | Meissa | 5:36:16 | 9.946 | 5:36:15 | 9.633 | Tarazed | 19:47:13 | 10.664 | 19:48:03 | 10.956 |
| Atik | 3:55:26 | 31.943 | 3:56:02 | 32.308 | Menkalinan | 6:01:02 | 44.947 | 6:02:00 | 45.163 | Tau Pup | 6:50:26 | -50.639 | 6:51:44 | -50.881 |
| Atlas | 3:50:23 | 24.115 | 3:52:10 | 24.502 | Menkent | 14:07:54 | -36.47 | 14:08:32 | -36.278 | Tejat | 6:24:10 | 22.501 | 6:25:56 | 22.131 |
| Azmidi | 7:50:09 | -24.912 | 7:49:44 | -25.013 | Merak | 11:03:04 | 56.27 | 11:01:51 | 55.911 | Tiaki | 22:43:51 | -46.778 | 22:43:07 | -46.585 |
| Bellatrix | 5:26:14 | 6.366 | 5:26:57 | 5.882 | Mintaka | 5:33:03 | -0.285 | 5:33:49 | -0.356 | Tianguan | 5:38:51 | 21.152 | 5:40:25 | 20.765 |
| Betelgeuse | 5:56:17 | 7.409 | 5:56:19 | 7.333 | Mirach | 1:10:53 | 35.729 | 1:11:44 | 35.261 | Tureis | 8:08:24 | -24.364 | 8:08:57 | -24.278 |
| Canopus | 6:24:24 | -52.707 | 6:23:13 | -52.957 | Mirfak | 3:25:48 | 49.933 | 3:26:56 | 50.262 | Vega | 18:37:38 | 38.804 | 18:37:35 | 38.849 |
| Capella | 5:18:13 | 46.016 | 5:19:01 | 46.167 | Mirzam | 6:23:36 | -17.967 | 6:24:00 | -17.66 | Wazn | 5:51:41 | -35.761 | 5:52:44 | -36.047 |
| Caph | 0:10:16 | 59.268 | 0:11:37 | 59.358 | Mizar | 13:24:45 | 54.817 | 13:22:50 | 54.707 | Wezen | 7:09:14 | -26.427 | 7:10:42 | -26.781 |
| Castor | 7:35:54 | 31.84 | 7:36:36 | 32.015 | Muhlifain | 12:42:40 | -49.072 | 12:43:48 | -48.885 | Zosma | 11:15:12 | 20.41 | 11:16:37 | 20.957 |

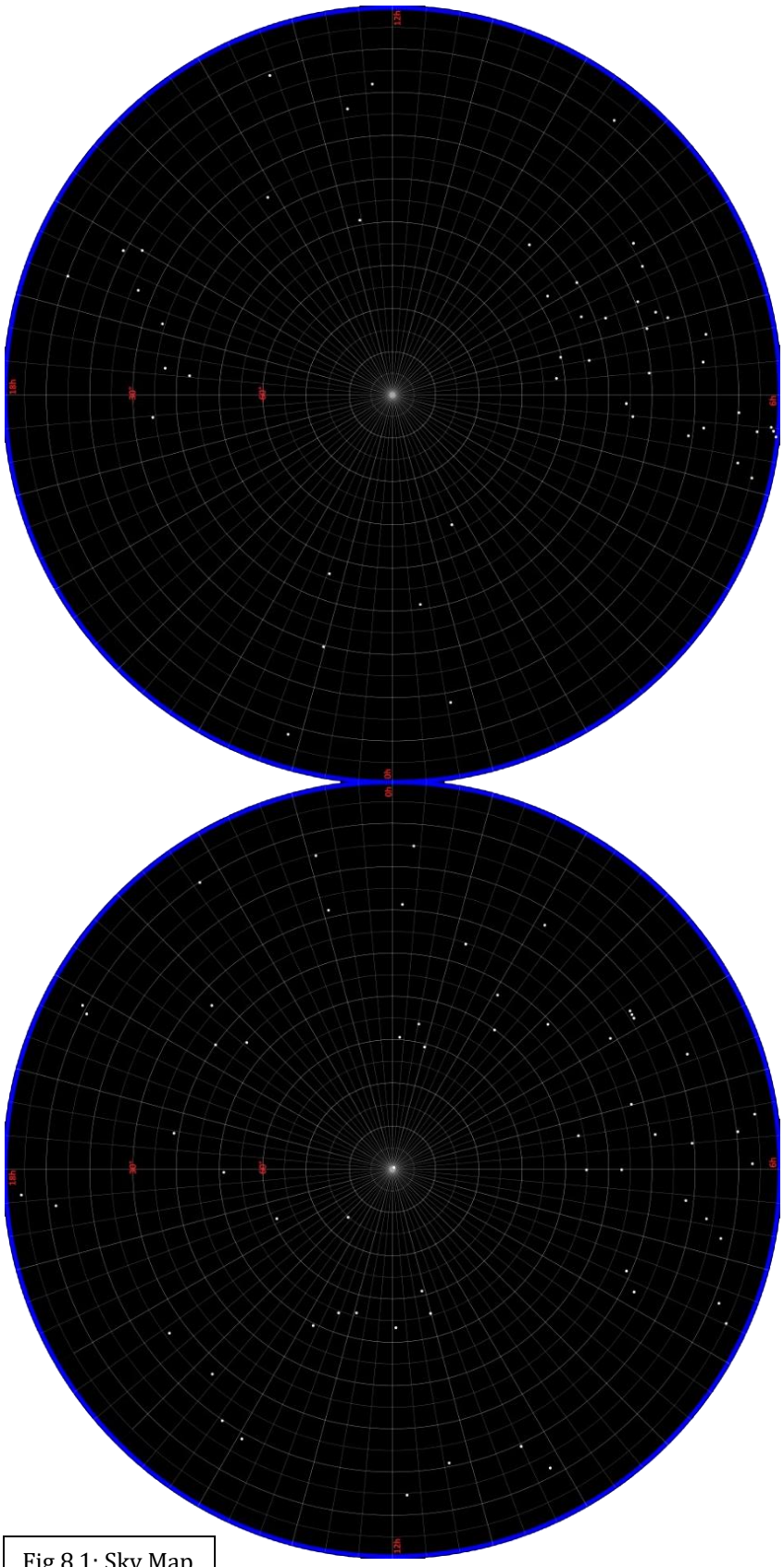

Fig 8.1: Sky Map

## Conclusion

The goals of the project included designing, building and testing an optical telescope and building a celestial mapping system that could be attached to the telescope. The goals of the project were almost met. An 8 inch f 8.8 parabolic mirror was modelled, ground and almost polished. There were difficulties encountered during polishing which prevented completion of telescope. However, the mirror was polished enough to subject it to various optical tests to study its surface profile and quality. The star test results corresponded with perfect a mirror. The Ronchi Wire test indicated the mirror to be a little overcorrected i.e. its conic constant was a little under -1 and therefor the surface was in the hyperboloid range. The Foucault knife edge test showed the mirror's conic constant to be -1.448 with a Strehl ratio of 0.95. The laser scattering test while polishing, did indicate a further 3-4 hours of polishing was needed for the perfect smooth finish.

The celestial mapping system was built using a Raspberry Pi and an Inertial Measurement Unit board. A python script was implemented to obtain mechanical orientation data from the sensors, use data on local coordinates and time and combine all of this data to output the celestial coordinates of the object to which the IMU board was pointed. This system was used to collect data on 108 stars, using already available telescopes, and the data was compared with that available online for the said stars. The collected data was also used to create a graphical sky map by projecting hemispherical data onto a circular grid.

Based on the experience obtained while working with the mirror, it is concluded that to complete the process of building the telescope, it is imperative to

thoroughly understand the composition of material which will be mixed to make the pitch lap. The lap will have to have proper viscosity so as to conform to the mirror perfectly during the process of pitch lap making. A perfect lap will allow the completion of the mirror polishing in a maximum of 3 to 4 hours of a polishing session. This will obviously result in the changing of the mirror surface, which can be retested using the test setup that was constructed for the purposes of this project. Once the result is satisfactory, the mirror can be sent to be aluminized and the telescope can be built.

The work on this project was an amazing addition to the undergraduate experience. The field was chosen to be able to learn about new concepts to which exposure had not previously been attained. Not only was it a great learning opportunity, first hand experience of things not working out the way they are intended to was seen. Many nights were spent collecting data on stars which turned out to match with actual data very closely thus showing the importance of patience and perseverance. At the end, the project was such, that as of today, I wouldn't want to change anything off, whether that be the successes or the failures during the processes.

## Appendix A: Python Code

The code that enabled the collection of celestial data consists of 4 Python Scripts. 3 of the scripts were adopted from the Github repository of the manufacturer of the IMU board. These scripts primarily deal with interfacing of the IMU board and the Raspberry Pi. The 4th script is the one that was designed as part of this project, although some portions of it were adapted and tweaked or customized for implementation into the final script. The following is the script that was designed for the project. Line 16, 17, 18 and 129 need to be changed based on user's physical location.

SkyMap.py

```
1.  import time
2.  import math
3.  import IMU
4.  import datetime
5.  import os
6.  import ephem
7.
8.
9.  IMU_UPSIDE_DOWN = 0
10.
11. RAD_TO_DEG = 57.29578
12. M_PI = 3.14159265358979323846
13. G_GAIN = 0.070
14. AA =  0.40
15.
16. lat = 12.85735
17. lon = 77.76175
18. localMagneticDeclination = 1.13
19.
20. magXmin =  -1005
21. magYmin =  348
22. magZmin =  -305
23. magXmax =  1170
24. magYmax =  2370
25. magZmax =  1786
26.
27. Q_angle = 0.02
28. Q_gyro = 0.0015
```

```
29.     R_angle = 0.005
30.     y_bias = 0.0
31.     x_bias = 0.0
32.     XP_00 = 0.0
33.     XP_01 = 0.0
34.     XP_10 = 0.0
35.     XP_11 = 0.0
36.     YP_00 = 0.0
37.     YP_01 = 0.0
38.     YP_10 = 0.0
39.     YP_11 = 0.0
40.     KFangleX = 0.0
41.     KFangleY = 0.0
42.
43.     def kalmanFilterY ( accAngle, gyroRate, DT):
44.       y=0.0
45.       S=0.0
46.
47.       global KFangleY
48.       global Q_angle
49.       global Q_gyro
50.       global y_bias
51.       global YP_00
52.       global YP_01
53.       global YP_10
54.       global YP_11
55.
56.       KFangleY = KFangleY + DT * (gyroRate - y_bias)
57.
58.       YP_00 = YP_00 + ( - DT * (YP_10 + YP_01) + Q_angle * DT )
59.       YP_01 = YP_01 + ( - DT * YP_11 )
60.       YP_10 = YP_10 + ( - DT * YP_11 )
61.       YP_11 = YP_11 + ( + Q_gyro * DT )
62.
63.       y = accAngle - KFangleY
64.       S = YP_00 + R_angle
65.       K_0 = YP_00 / S
66.       K_1 = YP_10 / S
67.
68.       KFangleY = KFangleY + ( K_0 * y )
69.       y_bias = y_bias + ( K_1 * y )
70.
71.       YP_00 = YP_00 - ( K_0 * YP_00 )
72.       YP_01 = YP_01 - ( K_0 * YP_01 )
73.       YP_10 = YP_10 - ( K_1 * YP_00 )
74.       YP_11 = YP_11 - ( K_1 * YP_01 )
75.
76.       return KFangleY
77.
78.     def kalmanFilterX ( accAngle, gyroRate, DT):
79.       x=0.0
80.       S=0.0
81.
82.       global KFangleX
83.       global Q_angle
```

```
84.         global Q_gyro
85.         global x_bias
86.         global XP_00
87.         global XP_01
88.         global XP_10
89.         global XP_11
90.
91.         KFangleX = KFangleX + DT * (gyroRate - x_bias)
92.
93.         XP_00 = XP_00 + ( - DT * (XP_10 + XP_01) + Q_angle * DT )
94.         XP_01 = XP_01 + ( - DT * XP_11 )
95.         XP_10 = XP_10 + ( - DT * XP_11 )
96.         XP_11 = XP_11 + ( + Q_gyro * DT )
97.
98.         x = accAngle - KFangleX
99.         S = XP_00 + R_angle
100.        K_0 = XP_00 / S
101.        K_1 = XP_10 / S
102.
103.        KFangleX = KFangleX + ( K_0 * x )
104.        x_bias = x_bias + ( K_1 * x )
105.
106.        XP_00 = XP_00 - ( K_0 * XP_00 )
107.        XP_01 = XP_01 - ( K_0 * XP_01 )
108.        XP_10 = XP_10 - ( K_1 * XP_00 )
109.        XP_11 = XP_11 - ( K_1 * XP_01 )
110.
111.        return KFangleX
112.
113.    IMU.detectIMU()
114.    IMU.initIMU()
115.
116.    gyroXangle = 0.0
117.    gyroYangle = 0.0
118.    gyroZangle = 0.0
119.    CFangleX = 0.0
120.    CFangleY = 0.0
121.    kalmanX = 0.0
122.    kalmanY = 0.0
123.
124.    a = datetime.datetime.now()
125.
126.    while True:
127.
128.        srtfunc = ephem.Observer()
129.        srtfunc.lon, srtfunc.lat = '77.76175', '12.85735'
130.
131.        ACCx = IMU.readACCx()
132.        ACCy = IMU.readACCy()
133.        ACCz = IMU.readACCz()
134.        GYRx = IMU.readGYRx()
135.        GYRy = IMU.readGYRy()
136.        GYRz = IMU.readGYRz()
137.        MAGx = IMU.readMAGx()
138.        MAGy = IMU.readMAGy()
```

```
        MAGz = IMU.readMAGz()

        MAGx -= (magXmin + magXmax) /2
        MAGy -= (magYmin + magYmax) /2
        MAGz -= (magZmin + magZmax) /2

        b = datetime.datetime.now() - a
        a = datetime.datetime.now()
        LP = b.microseconds/(1000000*1.0)

        rate_gyr_x =  GYRx * G_GAIN
        rate_gyr_y =  GYRy * G_GAIN
        rate_gyr_z =  GYRz * G_GAIN

        gyroXangle+=rate_gyr_x*LP
        gyroYangle+=rate_gyr_y*LP
        gyroZangle+=rate_gyr_z*LP

        if not IMU_UPSIDE_DOWN:
            AccXangle =  (math.atan2(ACCy,ACCz)*RAD_TO_DEG)
            AccYangle =  (math.atan2(ACCz,ACCx)+M_PI)*RAD_TO_DEG
        else:
            AccXangle =  (math.atan2(-ACCy,-ACCz)*RAD_TO_DEG)
            AccYangle =  (math.atan2(-ACCz,-ACCx)+M_PI)*RAD_TO_DEG

        if AccYangle > 90:
            AccYangle -= 270.0
        else:
            AccYangle += 90.0

        CFangleX=AA*(CFangleX+rate_gyr_x*LP) +(1 - AA) * AccXangle
        CFangleY=AA*(CFangleY+rate_gyr_y*LP) +(1 - AA) * AccYangle

        kalmanY = kalmanFilterY(AccYangle, rate_gyr_y,LP)
        kalmanX = kalmanFilterX(AccXangle, rate_gyr_x,LP)

        if IMU_UPSIDE_DOWN:
            MAGy = -MAGy

        heading = 180 * math.atan2(MAGy,MAGx)/M_PI

        if heading < 0:
            heading += 360

        if not IMU_UPSIDE_DOWN:
            accXnorm = ACCx/math.sqrt(ACCx * ACCx + ACCy * ACCy + ACCz * ACCz)
            accYnorm = ACCy/math.sqrt(ACCx * ACCx + ACCy * ACCy + ACCz * ACCz)
        else:
            accXnorm = -ACCx/math.sqrt(ACCx * ACCx + ACCy * ACCy + ACCz * ACCz)
            accYnorm = ACCy/math.sqrt(ACCx * ACCx + ACCy * ACCy + ACCz * ACCz)

        pitch = math.asin(accXnorm)
        roll = -math.asin(accYnorm/math.cos(pitch))

        magXcomp = MAGx*math.cos(pitch)+MAGz*math.sin(pitch)
```

```
194.
195.        if(IMU.LSM9DS0):
196.            magYcomp = MAGx*math.sin(roll)*math.sin(pitch)+MAGy*math.cos(roll)-
MAGz*math.sin(roll)*math.cos(pitch)
197.        else:
198.            magYcomp = MAGx*math.sin(roll)*math.sin(pitch)+MAGy*math.cos(roll)+MAGz*math
.sin(roll)*math.cos(pitch)
199.
200.        tiltCompensatedHeading = 180 * math.atan2(magYcomp,magXcomp)/M_PI
201.
202.        if tiltCompensatedHeading < 0:
203.            tiltCompensatedHeading += 360
204.
205.        alt = 90 - kalmanY
206.        az = tiltCompensatedHeading - localMagneticDeclination
207.        if az < 0:
208.        az += 360
209.
210.        if (az == 0):
211.            if (alt + lat) <= 90:
212.                Dec = alt + lat
213.                hadeg = 0
214.            else:
215.                Dec = 180 - (alt + lat)
216.                hadeg = 180
217.        elif (0 < az < 90):
218.            if ((lat + alt*math.sin(math.radians(90-az))) <= 90):
219.                Dec = (lat + alt*math.sin(math.radians(90-az)))
220.            else:
221.                Dec = 180 - (lat + alt*math.sin(math.radians(90-az)))
222.            hadeg = alt*math.cos(math.radians(90-az))
223.        elif (az == 90):
224.            Dec = lat
225.            hadeg = alt
226.        elif (90 < az < 180):
227.            if ((lat - alt*math.sin(math.radians(az-90))) >= -90):
228.                Dec = (lat - alt*math.sin(math.radians(az-90)))
229.            else:
230.                Dec = -180 - (lat - alt*math.sin(math.radians(az-90)))
231.            hadeg = alt*math.cos(math.radians(az-90))
232.        elif (az == 180):
233.            if ((lat - alt) > -90):
234.                Dec = lat - alt
235.                hadeg = 0
236.            else:
237.                Dec = -180 - (lat - alt)
238.                hadeg = 180
239.        elif (180 < az < 270):
240.            if ((lat - alt*math.sin(math.radians(270 - az))) >= -90):
241.                Dec = (lat - alt*math.sin(math.radians(270 - az)))
242.            else:
243.                Dec = -180 - (lat - alt*math.sin(math.radians(270 - az)))
244.            hadeg = - alt*math.cos(math.radians(270 - az))
245.        elif (az == 270):
246.            Dec = lat
```

```
247.            hadeg = - alt
248.         elif (270 < az < 360):
249.            if ((lat + alt*math.sin(math.radians(az-270))) <= 90):
250.               Dec = (lat + alt*math.sin(math.radians(az-270)))
251.            else:
252.               Dec = 180 - (lat + alt*math.sin(math.radians(az-270)))
253.            hadeg = - alt*math.cos(math.radians(az-270))
254.
255.         hahh = int(hadeg/15)
256.         if (hadeg >= 0):
257.         hamm = int(((hadeg%15)/15)*60)
258.         else:
259.         hamm = 60 - int(((hadeg%15)/15)*60)
260.         if (hadeg >= 0):
261.         hass = int(((hadeg%15)/15)*3600 - hamm*60)
262.         else:
263.         hass = 60 - int(((hadeg%15)/15)*3600 - int(((hadeg%15)/15)*60)*60)
264.         ahahh = abs(hahh)
265.
266.         dt = str(str(datetime.date.today())+' '+str(srtfunc.sidereal_time()))
267.         dt1 = datetime.datetime.strptime(dt, '%Y-%m-%d %H:%M:%S.%f')
268.
269.         if (hadeg >= 0):
270.         RA1 = dt1 + datetime.timedelta(hours=ahahh, minutes=hamm, seconds=hass)
271.         else:
272.         RA1 = dt1 - datetime.timedelta(hours=ahahh, minutes=hamm, seconds=hass)
273.
274.         RA = datetime.datetime.strftime(RA1, '%H:%M:%S')
275.
276.         print 'Dec:,',Dec,',','RA:,',RA
277.         print ""
278.
279.         time.sleep(0.03)
```

## Bibliography


Amateur Telescope Optics, n.d. https://telescope-optics.net/.

"ATM, Optics and DIY Forum." Cloudy Nights, n.d. https://www.cloudynights.com/forum/70-atm-optics-and-diy-forum/.

Bartels, Mel. Mel Bartels' Amateur Telescope Making, n.d. https://www.bbastrodesigns.com/tm.html.

"Improved Telescope Mounting." Science at Your Doorstep, February 15, 2018. https://scienceatyourdoorstep.com/2017/10/05/improved-telescope-mounting/.

Shankar, P. N. How to Build a Telescope. Bengaluru, Karnataka: Karnataka Rajya Vijnana Parishat, IISc, 1985.

Slater, Ken. "Amateur Telescope Making Main Page." Stellafane ATM Main Page, n.d. https://stellafane.org/tm/atm/index.html.

Texereau, Jean. How to Make a Telescope. Richmond, VA: Willmann-Bell, 1984.

Williams, Mark. "BerryIMU v2 - An Accelerometer, Gyroscope, Magnetometer and Barometric/Altitude Sensor." Ozzmaker, n.d. https://ozzmaker.com/product/berryimu-accelerometer-gyroscope-magnetometer-barometricaltitude-sensor/.

Williams, Mark. "BerryIMU." GitHub, n.d. https://github.com/ozzmaker/BerryIMU.